Journal of Organic and Pharmaceutical Chemistry

Review Article

OPEN ACCESS
Freely available online on
http://ophcj.nuph.edu.ua

UDC 547.97+535.34+535.37+544.164

V. M. Polishchuk, M. P. Shandura
Institute of Organic Chemistry of the National Academy of Sciences of Ukraine,
5, Akademika Kukharya str., Kyiv, 02094, Ukraine

Polymethine Dyes Based on 2,2-Difluoro-1,3,2-dioxaborine: A Minireview

Abstract

Aim. To summarize and analyze literature data on the polymethine dyes containing the 2,2-difluoro-1,3,2-dioxaborine ring.
Results and discussion. Boron difluoride complex of *β*-diketone (2,2-difluoro-1,3,2-dioxaborine, F_2DB) is a unique structural motif endowing organic compounds with prominent physicochemical properties, such as a strong fluorescence and high molar attenuation coefficients. Incorporation of the F_2DB core into a polymethine chromophore either as an end-group or as an integral part of the polymethine chain allows obtaining dyes with exceptional characteristics, highly appealing for design of up-to-date functional materials. This review focuses on the synthesis and spectral properties of the F_2DB-containing polymethines along with the latest advancement in the synthesis of highly fluorescent polyanionic polymethines. A brief discussion of the effects of the structural modification of the π-conjugated system on the photophysical properties of dyes is included.
Conclusions. The literature on the F_2DB-containing polymethines demonstrates a high potential of the F_2DB core for the development of strongly fluorescent and intensely absorbing dyes.
Keywords: dioxaborine; polymethine; merocyanine; anionic dye; absorption; fluorescence

В. М. Поліщук, М. П. Шандура
Інститут органічної хімії Національної академії наук України,
вул. Академіка Кухаря, 5, м. Київ, 02660, Україна

Поліметинові барвники на основі 2,2-дифлуоро-1,3,2-діоксаборину: міні-огляд

Анотація

Мета. Узагальнити та проаналізувати літературні дані про поліметинові барвники на основі 2,2-дифлуоро-1,3,2-діоксаборину.
Результати та їх обговорення. Бородифлуоридний комплекс *β*-дикетону (2,2-дифлуоро-1,3,2-діоксаборин, F_2DB) є унікальним структурним елементом, який надає органічним сполукам особливі фізико-хімічні властивості, такі, як сильна флуоресценція та високі коефіцієнти молярної екстинкції. Уведення ядра F_2DB до поліметинового хромофора як кінцевої групи чи як складової частини поліметинового ланцюга дає змогу отримувати барвники з винятковими характеристиками, привабливі для розробки сучасних функціональних матеріалів. У цьому огляді висвітлено питання синтезу та спектральних властивостей поліметинів, що містять ядро F_2DB, а також останні досягнення в синтезі високофлуоресцентних поліаніонних поліметинів. Додано коротке обговорення впливу структурних модифікацій π-спряженої системи на фотофізичні властивості барвників.
Висновки. Аналіз літератури про поліметини, що містять ядро F_2DB, свідчить про високий потенціал діоксаборинового комплексу для розробки барвників з яскравою флуоресценцією та інтенсивним світлопоглинанням.
Ключові слова: діоксаборин; поліметин; мероціанін; аніонний барвник; абсорбція; флуоресценція

Citation: Polishchuk, V. M.; Shandura, M. P. Polymethine Dyes Based on 2,2-Difluoro-1,3,2-dioxaborine: A Minireview. *Journal of Organic and Pharmaceutical Chemistry* **2022**, *20* (4), 27–53.
https://doi.org/10.24959/ophcj.22.271882
Received: *20 October 2022*; **Revised:** *5 December 2022*; **Accepted:** *12 December 2022*
Copyright© 2022, V. M. Polishchuk, M. P. Shandura. This is an open access article under the CC BY license (http://creativecommons.org/licenses/by/4.0).
Funding: The work is a part of the departmental research at Institute of Organic Chemistry of the NASU on the topic "Synthesis, structure, and photonics of the polymethine dyes with atypical chromophore systems" (the State registration No. 0117U003839; the research period – 2018–2022).
Conflict of interests: The authors have no conflict of interests to declare.

■ Introduction

Polymethines are arguably the most versatile class of organic dyes due to a broad viable range of structural fine-tuning that allows obtaining dyes with predetermined characteristics [1]. Numerous polymethine dyes of varying structure are reported to date, of which those bearing the 2,2-difluoro-1,3,2-dioxaborine ring have only recently gained a particular attention. The interest in dioxaborine-containing polymethines is mostly driven by their unique physicochemical properties, in particular, high molar attenuation coefficients (ε), a strong fluorescence in both visible and near-infrared (NIR) spectral regions, high stability in solutions and in the solid state. Accordingly, they became promising objects for applications in NLO materials [2–7], as fluorogenic probes for labeling of DNA [8], lipids [9, 10], and proteins [11, 12], as molecular rotors [13, 14], and as photosensitizers for a long-wavelength cationic photopolymerization [15].

This Perspective summarizes the advancements in research of the F_2DB-containing polymethines, as well as the fundamentals of their structure/property relationships. Dioxaborines bearing other than fluorine substituents at the boron atom, such as CN_2DB- or Ph_2DB-containing compounds [16, 17], are not included. The content is organized in regard to the position of the dioxaborine ring within the polymethine chromophore (as an end-group or as an integral part of the π-chain) and the electronic composition of the π-conjugated system (dipolar/quadrupolar merocyanines or anionic dyes). Although a short note regarding the applications of the F_2DB-containing polymethines is included, for more sophisticated discussion of the dioxaborine applications readers are encouraged to consult recent reviews [18–20].

■ Results and discussion

1. 2,2-Difluoro-1,3,2-dioxaborine

According to the IUPAC recommendations, the dioxaborine core, specifically, its betainic valence formulae, should be named as follows: 2,2-difluoro-1,3,2-oxaoxoniaborinine (Figure 1, compound **1**: $R^1 = R^2 = R^3 = H$). Nevertheless, the name "2,2-difluoro-1,3,2-dioxaborine" for the F_2DB complex, first introduced in 1969 [21] has got a wide acceptance. For simplicity, throughout this Perspective dubbings "dioxaborine" and "F_2DB" are consistently used, though no acronym for the 2,2-difluoro-1,3,2-dioxaborine core, (as "BODIPY" for compounds with the borondipyromethene core) has been established yet.

1.1. General synthetic methods

The ability of β-diketones to form coordination complexes with metalloids (boron, silicon, germanium, etc.) was demonstrated more than a century ago when the synthesis of the first boron β-diketonate complexes – bis(acetylacetone) boronium salts $[(C_5H_7O_2)_2B]AuCl_4$ and $[(C_5H_7O_2)_2B]PtCl_6$ – was reported [22]. These complexes were obtained by the reaction of acetylacetone with boron trichloride followed by the treatment of the intermediate $(C_5H_7O_2)_2BCl$ with tetrachloroaurate or hexachloroplatinate salts. However, boronium salts were not formed when boron trifluoride was used instead of BCl_3. The treatment of acetylacetone with boron trifluoride results in a substitution of only one fluorine atom, yielding the difluoroboron complex of acetylacetone (BF_2-acetylacetone) [23]. The report on obtaining BF_2-acetylacetone is the first account of the dioxaborine synthesis employing enolizable β-diketones and boron trifluoride. This method has since become the most common synthetic approach to dioxaborines (Scheme 1) [3, 23]. As for the synthesis of enolizable β-diketones, the synthetic methods varied broadly, from Claisen condensation to modern practices of using strong bases and a wide variety of both acylating agents and alkyl(aryl)substituted ketones [24, 25].

β-Diketones can also be synthesized through the Lewis base promoted acylation of aromatic compounds. Boron trifluoride as a Lewis base allows obtaining dioxaborines from aromatic compounds in one stage (Scheme 2) [26–42]. This method is particularly convenient for the synthesis of arylsubstituted and benzannelated dioxaborines.

4,5-Disubstituted dioxaborines can be obtained directly from epoxy(aryl)ketones though the ring-opening → rearrangement → BF_2-complexation sequence initiated by BF_3 (Scheme 3) [43–45]. Electron-donating substituents as R^1 and R^2 tend to accelerate the rearrangement, while electron-withdrawing ones slow it down.

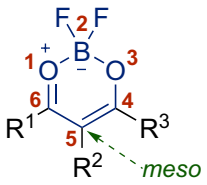

2,2-difluoro-1,3,2-dioxaborine

Figure 1. The structure of the F_2DB core

ISSN 2308-8303 (Print) / 2518-1548 (Online)

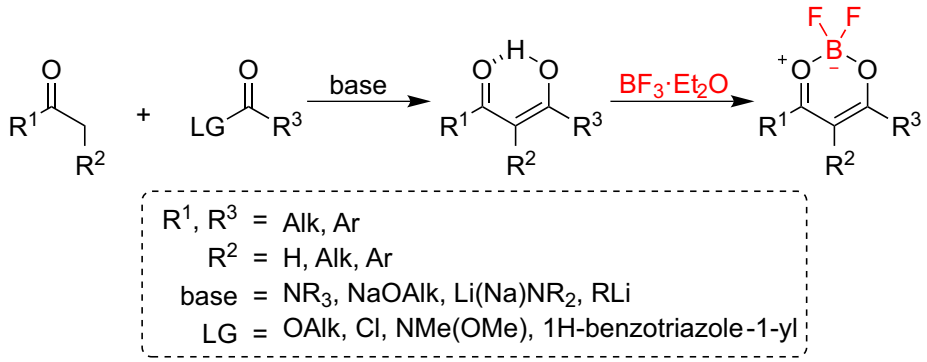

Scheme 1. The general approach to the dioxaborine synthesis

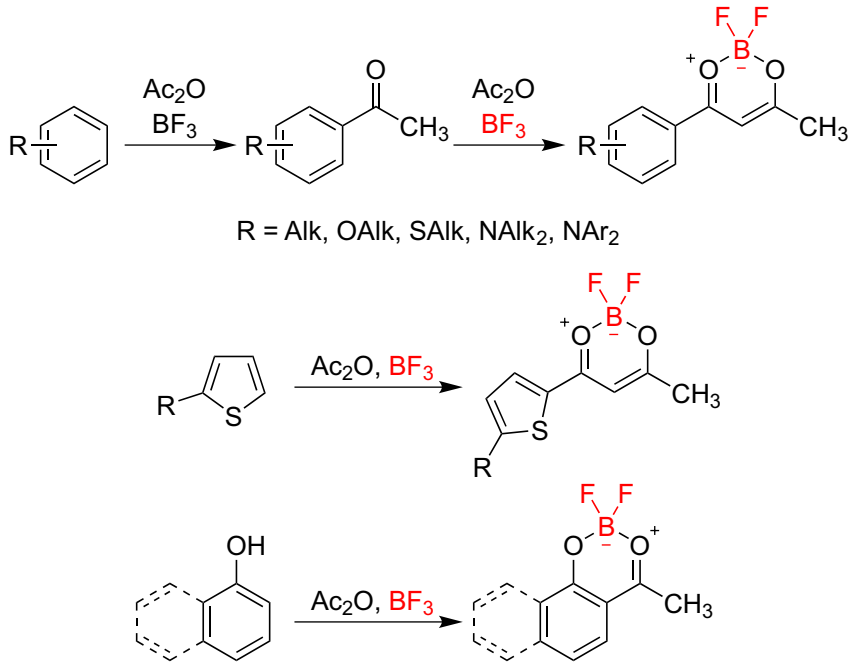

Scheme 2. Examples of the dioxaborine synthesis *via* the BF_3-promoted acylation of aromatics

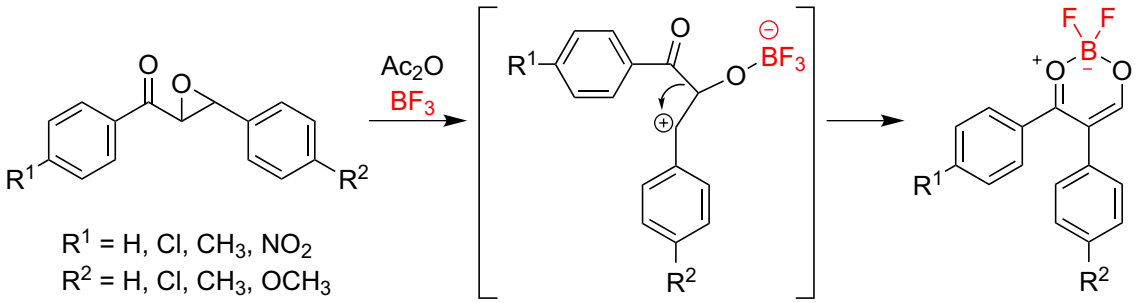

Scheme 3. The synthesis of dioxaborines through the rearrangement of epoxy(aryl)ketones

1.2. Fundamental properties

The 2,2-difluoro-1,3,2-dioxaborine complex is a donor-acceptor system constituting the *β*-diketonate ligand as an electron donor and boron difluoride as an electron acceptor (Figure 2, **a**). A dipolar character of the F_2DB core implies the high dipole moment, amounting to, for example, 7.6(±0.3) D and 6.7(±0.3) D in 1,4-dioxane for the BF_2-complexes of benzoylacetone and dibenzoylmethane, respectively [46]. Theoretical investigations suggest that the major contribution to such a strong polarization is the shift of the π-electron cloud of *β*-diketonate toward the acceptor BF_2 group (Figure 2, **b**: structure **C**) [47].

The depiction of the F_2DB core in a charge-separated resonance form can be misleading since a boron atom carries no negative charge. Analogously to inorganic borates (e.g., BF_4) [48], the negative charge is shifted to more electronegative fluorine atoms (Figure 2, **b**: structures **A** and **B**) [47].

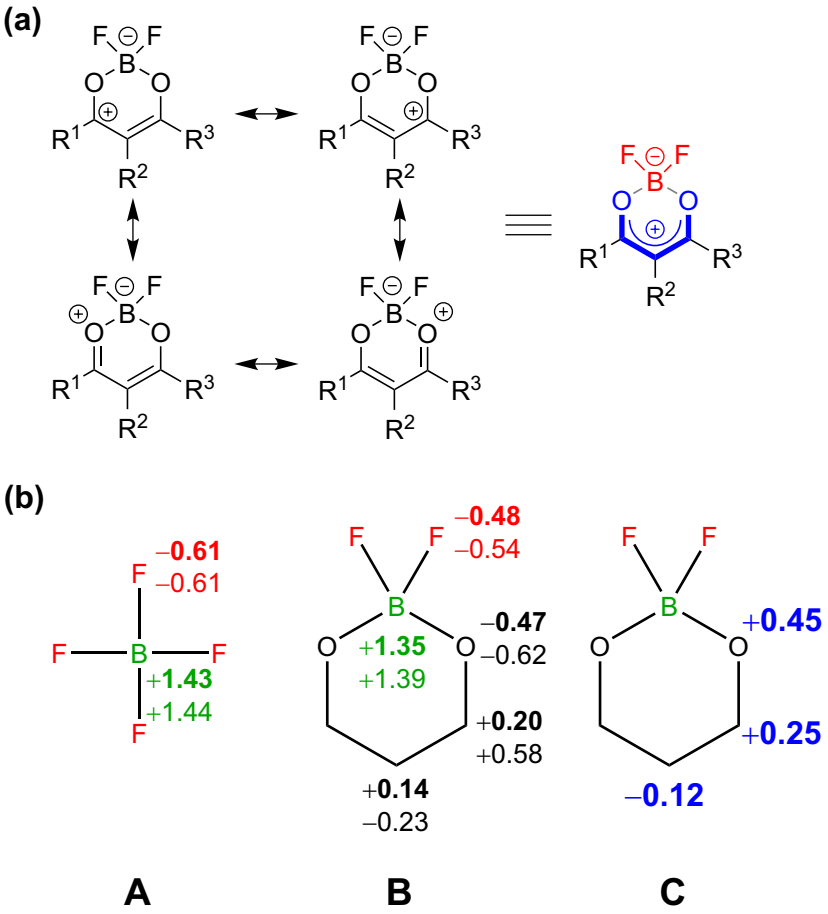

Figure 2. (a) The resonance forms of 2,2-difluoro-1,3,2-dioxaborine; (b) total charges of compound **1** (B) and tetrafluoroborate anion (A) according to the Mulliken population analysis (bold) and the natural population analysis (italics; DFT B3-LYP); charges of the π-system of **1** (C; Pariser–Parr–Pople approach)

Aromatic delocalization is not realized in the dioxaborine ring – the Nucleus-Independent Chemical Shift for **1** (Table 1) amounts to +2.3 ppm [47]. The calculated NICS implies negligible contribution of the BF_2 group into the cyclic delocalization (for the aromatic system, the NICS should be lesser than –3 ppm [49]). In addition, the quantum-chemical calculations have shown the $Bp_п$–$Op_п$ bonding is more than 4 times weaker than both $Op_п$–$C_αp_п$ and $C_αp_п$–$C_βp_п$ bonding, thus indicating the absence of the ring current. The results of the detailed investigation of the electronic structure of the dioxaborine core, including the energies and spatial distribution of the molecular orbitals, as well as the X-ray and spectral data of the simplest dioxaborines, are reported elsewhere [46, 47, 50–53].

The chelation of the *β*-diketonate structure by boron difluoride results in a substantial alteration of its properties. Closing of *β*-diketonate by the BF_2 group is usually accompanied by a bathochromic shift of the absorption maximum (λ^a_{max}) and an increase of the molar attenuation coefficient (ε). The magnitude of these effects is largely dependent on the structure of the parent

Table 1. Electron affinities of substituted dioxaborines calculated by DFT-B3LYP

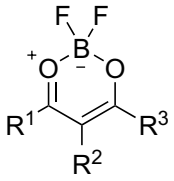

Compound	R^1	R^2	R^3	EA, eV[a]
1	H	H	H	0.97
2	CH_3	H	CH_3	0.63
3	CH_3	H	Ph	2.31
4	Ph	H	Ph	2.11
5	H	CN	H	1.81
6	CN	H	H	2.17
7	H	NO_2	H	1.8
8	NO_2	H	H	2.51
9	CF_3	H	CF_3	2.34
10	*p*-NO_2Ph	H	*p*-NO_2Ph	2.98
11	CN	H	CN	3.37
12	NO_2	H	NO_2	3.52

Note: [a] The EA value measures the ability of a neutral molecule (X) to gain an electron:

$$X + e^- \rightarrow X^- + EA$$

where EA is the energy released upon addition of an electron.

ISSN 2308-8303 (Print) / 2518-1548 (Online)

compound. For example, the absorption band of the BF_2-complex of acetylacetone lies 11 nm bathochromically and is twice as intense as that of acetylacetone (Figure 3), while for BF_2-curcumin the redshift vs. curcumin is much larger (see Figure 9). The downfield shift of the ^1H NMR signal of methyl groups of BF_2-acetylacetone complies with the electron-withdrawing effect of the BF_2 group on the *β*-diketonate scaffold [46].

The ^{19}F NMR spectra of dioxaborines do not conform with the theoretical model based on the properties of the ^{19}F, ^{10}B, ^{11}B nuclei. Considering the number of B nuclei (n) in *2nI+1* is one and nuclear spins (*I*) of ^{10}B and ^{11}B are equal to 3 and 3/2, respectively, the ^{11}B–^{19}F coupling should lead to an appearance of a quartet (1:1:1:1 intensity ratio), while the ^{10}B–^{19}F coupling should result in a heptet (1:1:1:1:1:1:1). Instead, the ^{19}F NMR spectra of compounds containing the F_2DB unit usually comprise a doublet with the intensity ratio of 1:4, reflecting the natural abundances of ^{10}B (19.09%) and ^{11}B (80.1%) isotopes [54]. Interestingly, such a coupling-deprived pattern with different resonance frequencies of ^{19}F atom bonded to ^{10}B and ^{11}B is also observed for $AgBF_4$ in 80% aqueous acetonitrile [55]. The absence of ^{11}B–^{19}F and ^{10}B–^{19}F coupling has not been conclusively explained so far; a suggestion of the rapid quadrupolar relaxation of the boron nuclear-spin states, which effectively decouples the boron from the fluorine nuclei, is debunked experimentally by examining their ^{11}B resonance [46]. In contrast to dioxaborines, BODIPYs are characterized by the appearance of a quartet in their ^{19}F NMR spectra reflecting the ^{11}B–^{19}F coupling (the ^{10}B–^{19}F coupling pattern is rarely visible due to a low abundance of the ^{10}B isotope and its small magnetogyric ratio, though for compounds with inequivalent fluorine atoms such a pattern can be spotted [56]).

As was described above, the electron-accepting nature of the dioxaborine core results from the withdrawal of the π-electron cloud from *β*-diketonate towards BF_2, thus making the OCCCO scaffold electron deficient. Modulation of the accepting strength can be achieved through the introduction of various substituents at positions 4, 5, and 6 of the dioxaborine scaffold. As a quantitative measure of the accepting strength, a molecular electron affinity (EA) can be used (Table 1) [47, 57]. Thus, considering the calculated values of EA, unsubstituted dioxaborine complex **1** is an acceptor of a moderate strength (EA = 0.97 eV) comparable to nitrobenzene (EA = 1.00 eV [58]). The insertion of one strong electron-withdrawing substituent into a *β*-diketonate backbone, such as CN or NO_2, doubles the magnitude of EA (compounds **5**–**8**), while the *bis*-substitution into positions 4 and 6 makes the F_2DB core a strong acceptor (compounds **9**–**12**) comparable to tetracyanoethylene (EA = 3.17 eV [59]).

1.3. Simple dioxaborine-containing π-conjugated systems

Although BF_2-acetylacetone absorbs in the near UV region (Figure 3), its absorption maximum can be red-shifted via the substitution of methyl groups with other alkyl or aryl groups. For example, the replacement of both CH_3 by *tert*-butyls results in a 10 nm bathochromic shift and a slight increase of the molar absorptivity due to hyperconjugation (Table 2) [46]. Extending the effective length of the conjugated π-system by the introduction of unsubstituted phenyl rings results in larger bathochromic shifts ($\Delta\lambda^a_{max}$ = 47 nm when **2** → **3** and 35 nm when **3** → **4**).

The absorption bands of the arylsubstituted dioxaborines have several maxima attributed to different electronic transitions. The DFT calculations ascribed the long-wavelength band (328–365 nm) of compounds **3**, **4**, **15**–**17** to the $^1\pi$–π^* excitation delocalized within the whole molecule, while the short-wavelength peak (265–270 nm) was linked to the redistribution of the electron density from aromatic substituents to the F_2DB core (light-induced intermolecular charge transfer) [51, 52].

The introduction of electron-donating substituents (methoxy or dialkylamine) into the *para*-position of the phenyl ring of compound **3** leads to a substantial redshift of the absorption maximum and large increase of the fluorescence intensity (Table 3) [60]. The reasoning behind such spectral changes is not only due to an enhancement of the intermolecular charge transfer, but

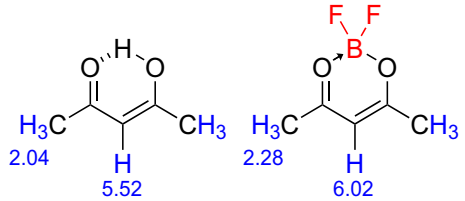

λ^a_{max} =	272 nm	283 nm
ε [M^{-1} cm^{-1}] =	8500	16980

Figure 3. The impact of the BF_2-chelation of acetylacetone on the spectral properties (NMR data in $CDCl_3$; λ^a_{max} and ε in $CHCl_3$ as the solvent)

Table 2. Characteristics of the UV absorption spectra of simple dioxaborines in $CHCl_3$

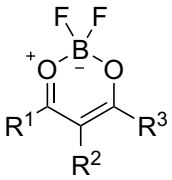

Compound	R^1	R^2	R^3	λ^a_{max} [nm]	log(ε)
2	CH_3	H	CH_3	283	4.23
3	CH_3	H	Ph	265, 328, 342	3.69, 4.47, 4.29
4	Ph	H	Ph	270, 365, 378	3.69, 4.62, 4.57
13	CH_3	H	*t*-Bu	289	4.26
14	*t*Bu	H	*t*-Bu	293	4.35
15	*n*Pr	H	Ph	265, 330, 346	3.69, 4.51, 4.35
16	*i*Pr	H	Ph	265, 333, 346	3.69, 4.50, 4.32
17	*t*Bu	H	Ph	265, 332, 346	3.69, 4.49, 4.33
18	2-pyridyl	H	Ph	368, 385	4.54, 4.49
19	2-thienyl	H	CF_3	325, 365	4.27, 4.37
20	CH_3	CH_3	CH_3	304	4.19
21	CH_3	CH_3	Ph	260, 334	3.65, 4.36
22	Ph	CH_3	Ph	260, 360	3.65, 4.48

Table 3. Spectral properties of compounds **3**, **23**, and **24** in $CHCl_3$ and MeCN

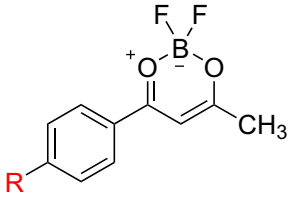

R = H OMe NMe_2

3 **23** **24**

Compound	Solvent	λ^a_{max} [nm]	$\varepsilon \times 10^{-4}$ [M^{-1} cm^{-1}]	λ^f_{max} [nm]	Φ_f	$\Delta\nu_s$ [cm^{-1}]
3	$CHCl_3$	328	2.95	382	$9 \cdot 10^{-4}$	4310
	CH_3CN	328	2.69	–	–	–
23	$CHCl_3$	359	4.57	388	0.37	2080
	CH_3CN	356	–	399	0.27	3030
24	$CHCl_3$	422	2.88	463	0.45	2100
	CH_3CN	423	–	485	$1 \cdot 10^{-3}$	3020

also due to the incorporation of an additional electron pair from O- and N-atom to the π-system, thus slightly expanding the effective conjugation length and altering its electronic structure.

The fluorescence intensity of compound **3** can also be increased by hindering free rotation of the phenyl ring around the bond linking it to the F_2DB core. For instance, the insertion of $–CH_2–CH_2–$ and –C(O)–O– bridges via the *ortho*-position of the phenyl ring and position 5 of the F_2DB core leads to a substantial increase of the fluorescence intensity (820-fold for **3** → **25** and 102-fold for **3** → **27**; Table 4) [32, 60]. Further insertion of methoxy or dialkylamino groups into the *para*-position of the phenyl ring greatly increases the molar absorptivity (compounds **26** and **28**).

Benzannelation of the phenyl ring of compound **3** results in a redshift of λ^a_{max}, a significant increase of ε, and a considerable fluorescence enhancement (**3** → **29**; Table 4) [61]. The replacement of the naphthyl substituent with 3-coumarinyl (**29** → **30**) shifts the absorption maximum bathochromically by 37 nm, while the molar absorptivity drops drastically, and the fluorescence is nearly quenched [32]. Expectedly, the introduction of a dialkylamino group into the *para*-position of the phenyl ring (**30** → **32**) induces both a large redshift of λ^a_{max} and an increase of the fluorescence quantum yield. Note that dioxaborine **32** is characterized by an exceptionally high molar attenuation coefficient (ε = 98500 M^{-1} cm^{-1} in DCM) compared to other simple dioxaborines.

ISSN 2308-8303 (Print) / 2518-1548 (Online)

Table 4. Optical properties of dyes **25**–**32** in dichloromethane (DCM)

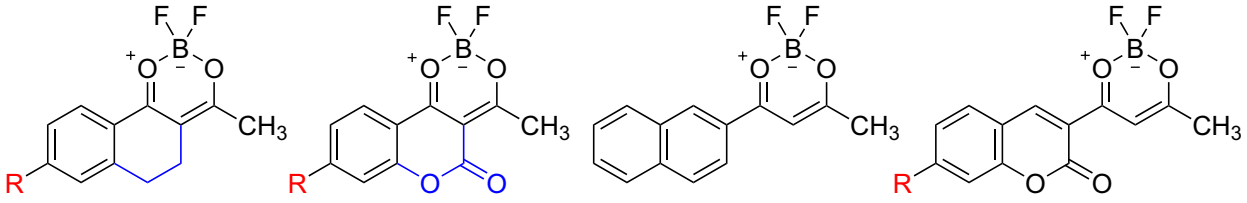

Compound	λ^{a}_{max} [nm]	$\varepsilon \times 10^{-4}$ [M^{-1} cm^{-1}]	λ^{f}_{max} [nm]	Φ_f	$\Delta\nu_s$ [cm^{-1}]
25	360	2.09	418	0.74	3850
26	383	3.63	414	0.69	1960
27	343	0.87	423	0.092	5510
28	424	5.68	465	0.11	2080
29	344	3.43	–	0.63	–
	380[a]	0.99[a]	459	–	4530
30	381	2.97	489	0.094	5800
31	385	2.70	443	0.23	3400
32	498	9.85	532	0.78	1280

Note: [a] shoulder

2. Dioxaborine as an end-group of the polymethine dyes

Polymethine dyes constituting the F_2DB core as an end-group (A) can be divided into neutral dipolar compounds of the A–π–D type (also known as merocyanines [62]; D is the electron donor end-group) and anionic symmetric (A–π–A) or non-symmetric (A–π–A') dyes (Figure 4).

The electronic structure of polymethine dyes in the ground state S_0 can be rendered as superposition of two boundary states: (*i*) polyene state, which is characterized by low degree of π-delocalization and a considerable alternation of the single and double bonds along the π-chain; and (*ii*) ideal polymethine state (or cyanine-like state [1, 63]) where π-delocalization is of the highest degree with no alternation of the bond orders along the π-chain [64]. The contribution of each of these states to the resulting electronic structure of a dye in the ground state S_0 is dependent on the structure of the end-groups and the length of the polymethine chain. The qualitative assessment of their relative contribution can be made on the grounds of spectral properties of a polymethine dye. An approach to the ideal polymethine state is usually accompanied by a narrowing of the absorption and emission bands, an increase of the molar absorptivity, and enhancement of the fluorescence intensity [65–67]. Taking into account these considerations the dioxaborine-containing merocyanines can be divided into two types of scaffolds depending on the electron-donating power of the end-group – type I containing weakly electron-donating *para*-(dialkyl(aryl)amino)phenyl or *para*-alkoxyphenyl end-groups, and type II dyes with stronger electrondonating end-groups (e. g., benzannelated heterocycles). Generally, the electronic structure of type II F_2DB-merocyanines is more closely approaching the ideal polymethine state when compared to type I dyes.

2.1. Synthesis of merocyanines and anionic polymethines

Most of the documented F_2DB-merocyanines of type I contain end-group *para*-alkoxy- or *para*-dialkylamino-substituted aromatic rings as an electron donor. These compounds can be prepared

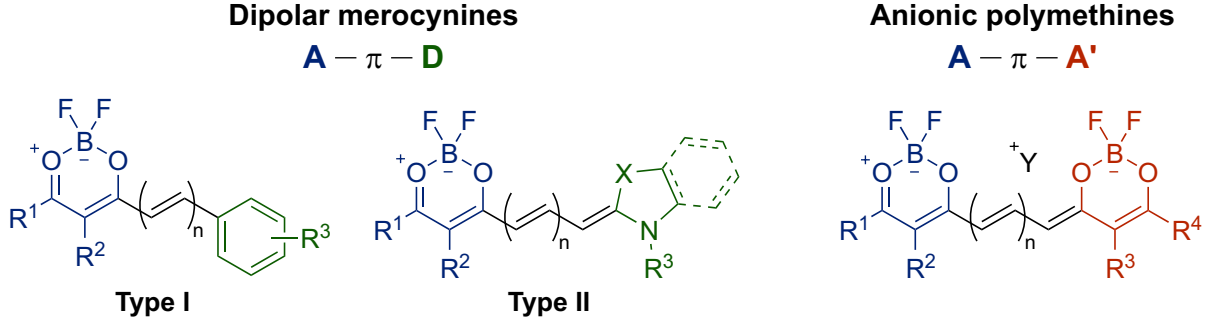

Figure 4. The general structures of merocyanines and anionic dyes containing the F_2DB core as an end-group

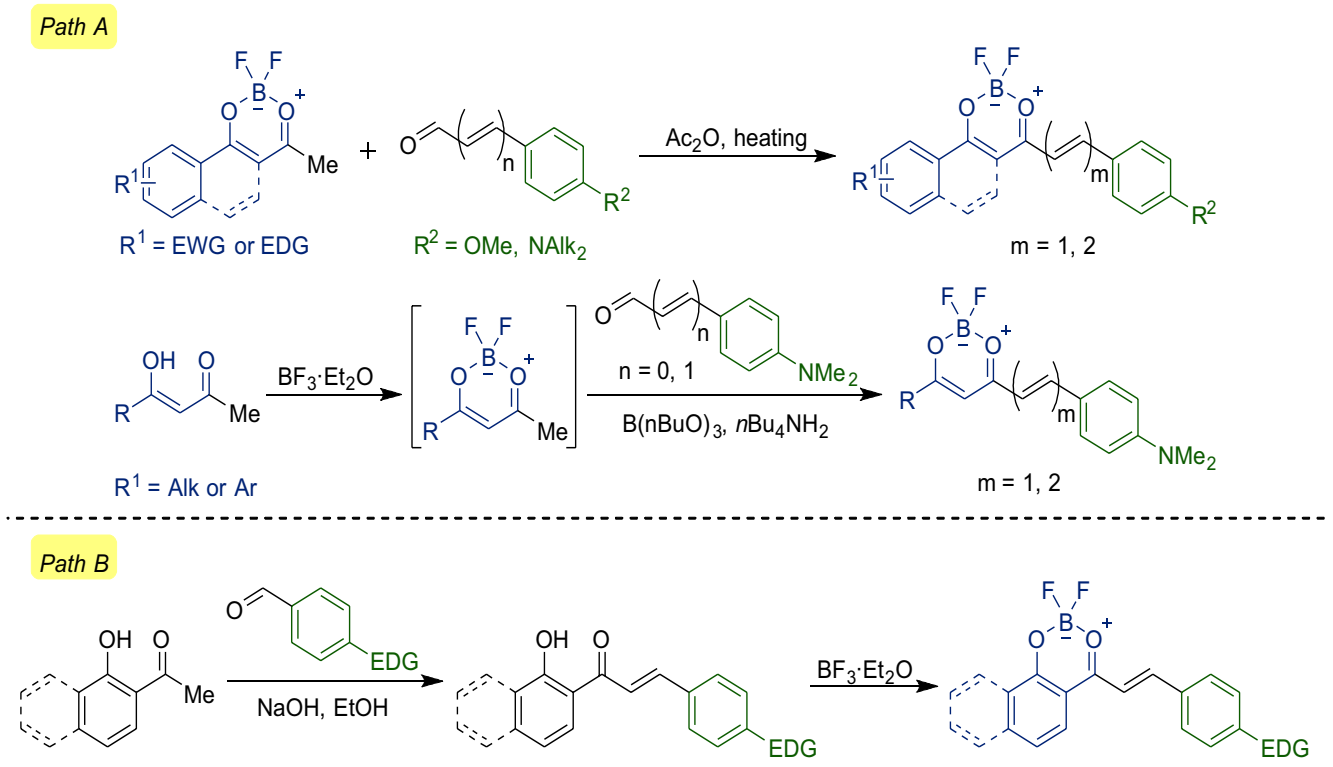

Scheme 4. The synthesis of type I F_2DB-containing merocyanines

by (I) condensation of methyl-substituted dioxaborines with benzaldehydes or cinnamic aldehydes when heating in acetic anhydride (Scheme 4, *Path A*) [2, 10, 21, 68, 69], or (II) aldol condensation of *ortho*-hydroxyphenones with benzaldehydes followed by treating with trifluoroborate etherate (Scheme 4, *Path B*) [70, 71]. The modification of the first method includes the initial *in situ* synthesis of the dioxaborine core from *β*-diketonate and $BF_3 \cdot Et_2O$ and further treatment of the intermediate compound with cinnamaldehyde in the presence of trialkylborate and *n*-butylamine [72].

The electron donor group of type II dipolar polymethines with the F_2DB core is represented by benzannelated heterocycles, such as *N*-alkyl-3,3-dimethylindolenine, *N*-alkylquinoline or *N*-alkyl-benzothiazole. Similarly to type I polymethines, these dyes can also be synthesized from methyl-substituted dioxaborines and unsaturated aldehydes when heating in acetic anhydride (Scheme 5, *Path A*) [73–77]. Instead of aldehydes, cationic hemicyanines can be used as an electrophilic substrate (Scheme 5, *Path B*) [74].

Neutral hemicyanines derived from dioxaborines are also suitable electrophilic reagents for the synthesis of dioxaborine-containing merocyanines. The two-step synthetic sequence involves the condensation of methyl substituted dioxaborines with dimethylformamide [73, 77], ethyl isoformanilide [74], dianils of malondialdehyde [9, 11, 74, 77, 78] or glutaconaldehyde [9] followed by the reaction of the obtained hemicyanines with quaternary heterocyclic salts (Scheme 5, *Path C*).

Symmetric anionic dioxaborine-containing polymethines can be synthesized in one stage from methyl-substituted dioxaborine and triethyl orthoformate [73, 79, 80], acrolein diethyl acetal [79], dianils of malondialdehyde [6] or glutaconaldehyde [78, 81], salts of 1,7-*bis*(dimethylamino) hepta-1,3,5-trienes [3, 6] in the presence of a base and acetic anhydride (Scheme 6, *Path A*). Polymethines with functional groups in the polymethine chain can be obtained similarly via the condensation of functionalized iminium salts with dioxaborine nucleophiles [3, 5, 79, 80, 82]. An alternative path to F_2DB-containing anionic dyes includes the two-stage sequence starting from the F_2DB-containing hemicyanine synthesis and subsequent condensation of the obtained intermediate with the nucleophile (Scheme 6, *Path B*) [78]. By this method non-symmetric dyes can be obtained [83].

2.3. Spectral properties of dioxaborine-containing merocyanines

Dipolar type I F_2DB-merocyanines are characterized by absorption in the visible region (400–650 nm). The bathochromic shift upon extending of the polymethine chain by one vinylene group (vinylene shift) amounts to nearly 50 nm (50 nm for **36** → **38** in MeCN or 42 nm for **39** → **40**

ISSN 2308-8303 (Print) / 2518-1548 (Online)

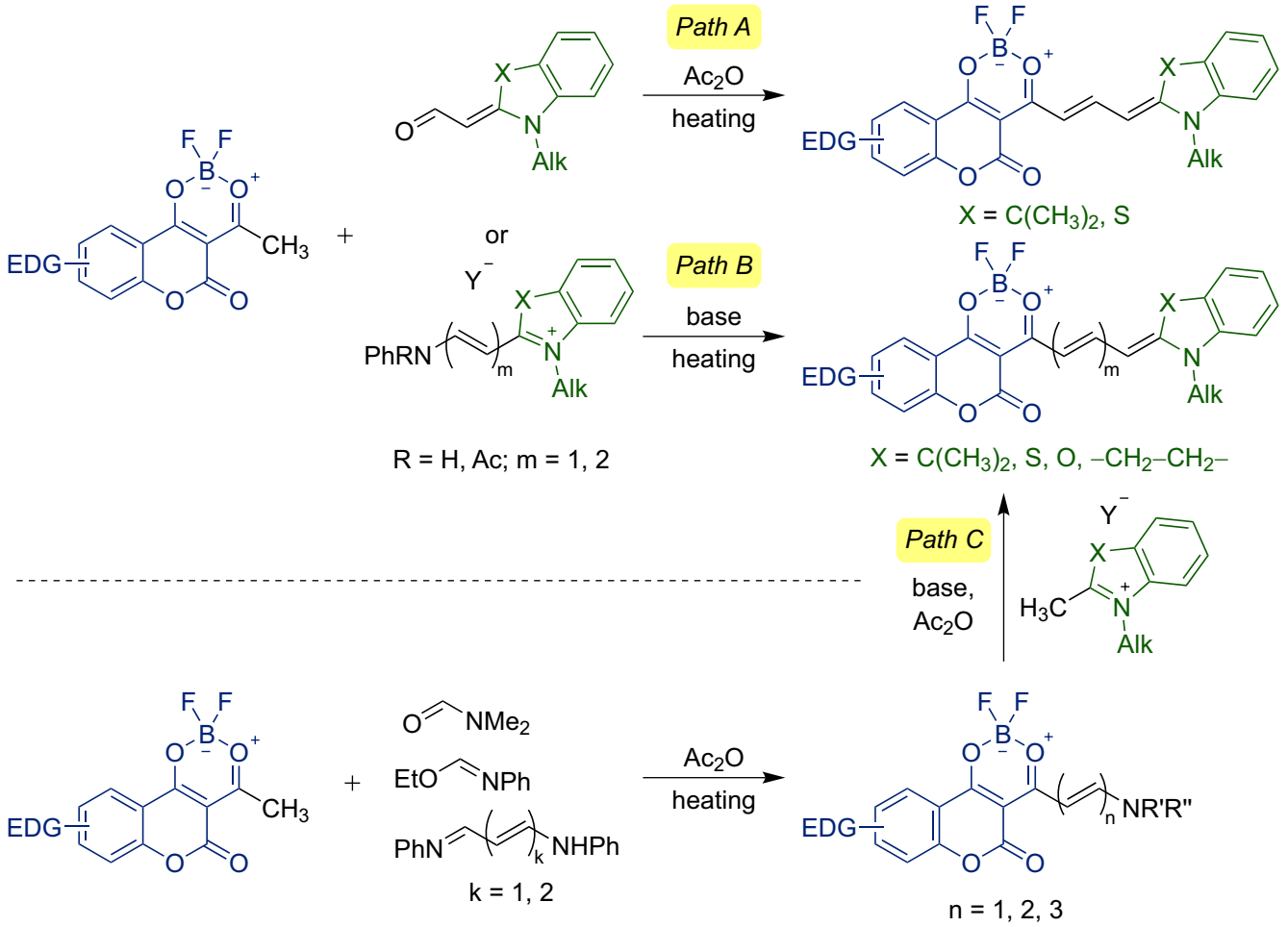

Scheme 5. The synthesis of type II F_2DB-containing merocyanines

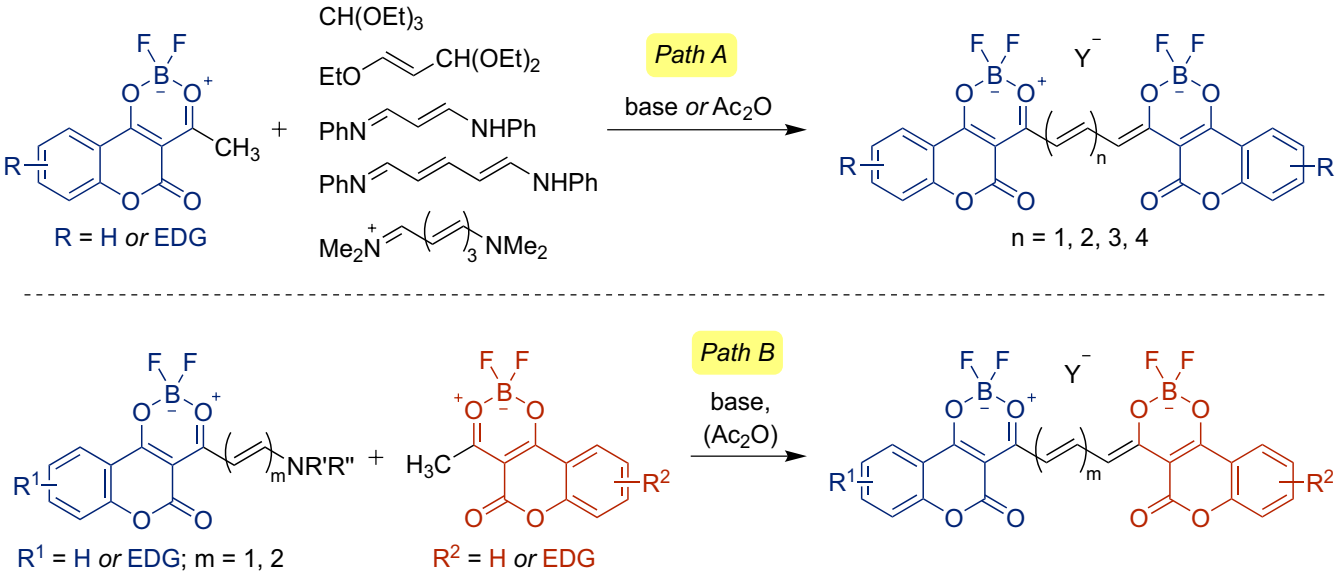

Scheme 6. The synthesis of symmetric and asymmetric F_2DB-containing anionic polymethines

in 1,2-dichloroethane; Tables 5 and 6) [21, 69], while for the dye with a diethylamine end-group vinylene shift reaches 84 nm in MeCN (**33** → **34**). Considering that the vinylene shift of symmetric cyanine dyes – polymethines, which approach the ideal polymethine state in the ground state S_0, – reaches 100 nm [63], such a low vinylene shift of type I F_2DB-merocyaniens marks their polyenic-like electronic structure.

In addition to the lengthening of the π-chain, the structural modification of the electron donor end-group can also yield a significant bathochromic

Table 5. Spectral properties of type I F_2DB-merocyanines in $CHCl_3$

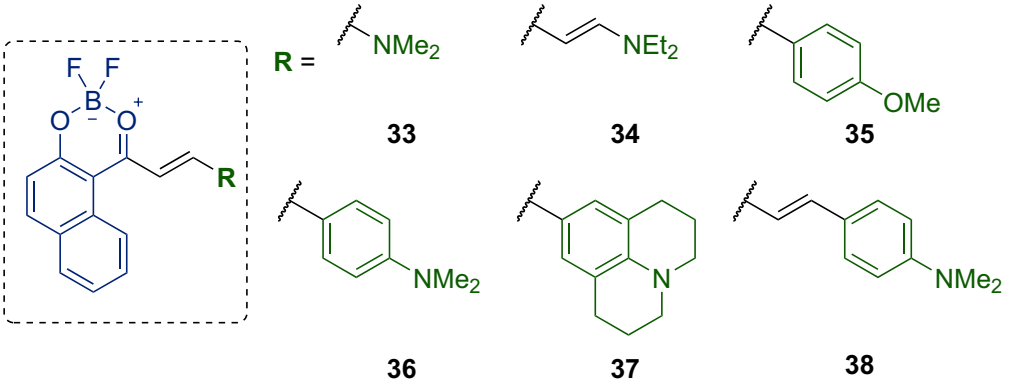

Compound	λ^a_{max} [nm] ($\varepsilon \times 10^{-4}$ [M^{-1} cm^{-1}])		
33	245 (*2.38*)	412 (*3.12*)	428 (*2.76*)
34	240 (*1.35*)	484 (*5.47*)	512 (*5.78*)
35	224 (*4.36*)	374 (*1.24*)	470 (*2.10*)
36	252 (*1.08*)	–	570 (*7.2*)
37	–	–	610 (*6.3*)
38	230 (*3.0*)	–	620 (*5.55*)

Table 6. Optical properties of dyes **39** and **40** in various solvents

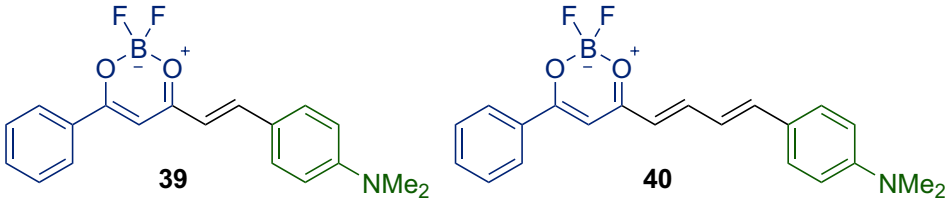

Compound	Solvent	λ^a_{max} [nm]	λ^f_{max} [nm]	Φ_f
39	toluene	519	571	0.8
	1,2-dichloroethane	536	635	0.025
	DMSO	553	660	0.002
40	toluene	555	640	0.35
	1,2-dichloroethane	578	712	0.071
	DMSO	580	770	0.003

shift. For instance, the replacement of the methoxy by a dialkylamino group leads to a 100 nm redshift of λ^a_{max} (**35** → **36** in MeCN) and a three-fold increase of the molar absorptivity. The fluorescence quantum yield of 4-(dialkylamino)phenyl-containing polymethines is also exceptionally high as for polymethine dyes (0.8 in toluene for dye **39**). The fluorescence intensity of the type I F_2DB-containing merocyanines significantly decreases with a decrease of the solvent polarity. Such sensitivity to the environment polarity stimulated an extensive research on dimethine- and tetramethine-bridged donor-acceptor systems as fluorescent probes for bioimaging [10, 72, 84–88].

Merocyanines bearing the BF_2-complex of 8-(dialkylamino)-3-acetyl-4-hydroxycoumarin have outstanding spectral properties among the type I F_2DB-merocyanines, such as a high molar extinction coefficient and a strong fluorescence (Table 7) [10, 14]. Similar to compounds **39** and **40**, dyes **41** and **42** are characterized by a high sensitivity of the fluorescence intensity to the solvent polarity. Besides, dyes **41** and **42** possess the highest molar absorption coefficients among the type I F_2DB-merocyanines.

Non-linear optical properties of several type I F_2DB-merocyanines have also been evaluated. The electro-optic coefficient r_{33}, as well as the product of the ground state dipole moment and the first hyperpolarizability $\mu\beta$ can be adjusted in a broad range via the structural modification of the phenyl ring of the dioxaborine end-group. For instance, the introduction of the NO_2 group into the *para*-position of the phenyl ring of the dioxaborine core results in a three-fold increase of the $\mu\beta$ magnitude (**45** → **46**; Table 8) [2]. Lengthening of the π-chain by one vinylene group induces a two-fold increase of r_{33} and $\mu\beta$

ISSN 2308-8303 (Print) / 2518-1548 (Online)

Table 7. Spectral properties of polymethines **41** and **42**

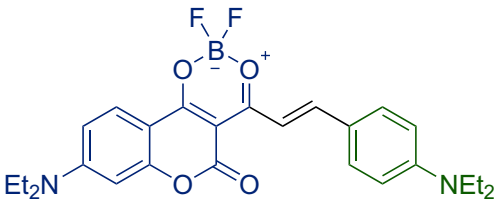

41

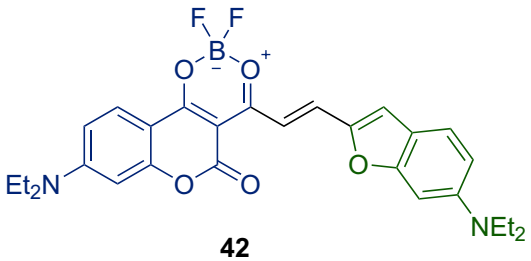

42

Compound	Solvent	λ^{a}_{max} [nm]	$\varepsilon \times 10^{-4}$ [M^{-1} cm^{-1}]	λ^{f}_{max} [nm]	Φ_f
41	cyclohexane	542	–	556	0.46
	toluene	567	–	597	0.93
	ethanol	581	12.0	635	0.044
	DMSO	607	–	659	0.035
42	cyclohexane	602	12.8	622	0.93
	toluene	627	–	687	0.81
	ethanol	645	12.3	748	0.18
	DMSO	678	9.3	778	0.03

Table 8. Non-linear optical properties of type I F_2DB-merocyanines

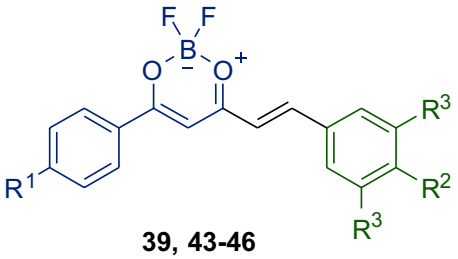

39, 43-46

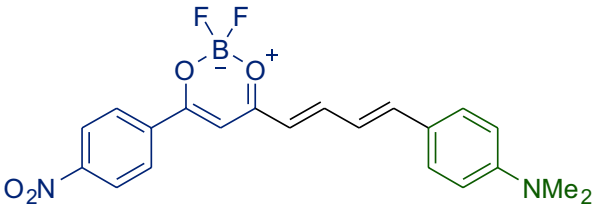

47

Compound	R^1	R^2	R^3	λ^{a}_{max} ($CHCl_3$) [nm]	r_{33} [nm V^{-1}]	$\mu\beta \times 10^{-48}$ [esu]
39	H	NMe_2	H	530	1.98	364
43	OMe	NEt_2	H	538	1.57	284
44	F	NBu_2	H	546	2.97	514
45	H	–N–	$–(CH_2)_3–$	570	3.26	512
46	NO_2	–N–	$–(CH_2)_3–$	609	11.4	1400
47	NO_2	NMe_2	H	614	23.64	3150

values (**46** → **47**), thus rendering dye **47** and its derivatives promising objects for non-linear optical devices.

In contrast to type I dyes, type II F_2DB-merocyanines absorb not only in the visible region, but also in the near-infrared (Table 9). While type I dyes have a moderate magnitude of ε, the molar absorbance of type II dyes is typically nearly twice as intense and often exceeds the value of 200000 M^{-1} cm^{-1} in the band maximum [78]. Vinylene shifts are also larger for type II polymethines, reaching 100 nm (e.g., **56** → **50**). These properties along with sharp absorption bands imply a high similarity of the ground S_0 and excited S_1 states of type II F_2DB-merocyanines, thus indicating an effective delocalization of the π-electrons along the chromophore. Interestingly, a decrease of the accepting strength of the dioxaborine core by insertion of dialkylamino substituents into the aromatic ring (**48** → **51** → **57**) enhances stability of the dyes toward the hydrolytic cleavage of the boron difluoride group [75].

In addition to type II polymethines designed from the BF_2-complex of 3-acetylcoumarin, merocyanines derived from the BF_2-complex of 5-acetylbarbituric acid (**58–63**) are also characterized by notable spectral properties [9]. For example, the molar absorptivity for dye **60** reaches 363000 M^{-1} cm^{-1} in DMSO, while dye **62** intensely fluoresces in the NIR region (λ^{f}_{max} = 779 nm and Φ_f = 0.33 in DMSO). Moreover, the fluorescence brightness ($\varepsilon \times \Phi_f$) of dye **60** amounts to 152000 M^{-1} cm^{-1}, which is one of the highest magnitudes among merocyanines. These dyes also possess prominent non-linear optical properties, making them suitable candidates for application in two-photon excitation microscopy.

Table 9. Spectral properties of type II F_2DB-merocyanines in $CHCl_3$

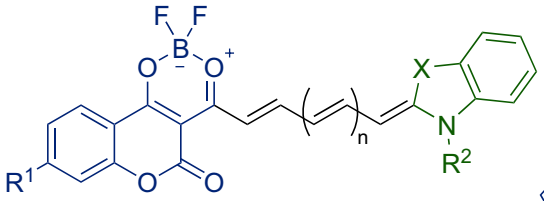

48, 50-56

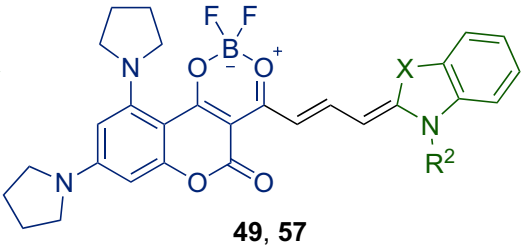

49, **57**

Dye	X	n	R^1	R^2	λ^a_{max} [nm]	$\varepsilon \times 10^{-5}$ [M^{-1} cm^{-1}]	λ^f_{max} [nm]	Φ_f	$t_{0.5}$[a] [s]	k[b] [s^{-1}]
48	$C(CH_3)_2$	0	H	Me	569	1.49	590	0.03	50	1.40×10^{-2}
49	S	–	–	Me	601	–	620	0.49	–	–
50	CH=CH	1	NEt_2	Bu	721	3.15	729	–	–	–
51	$C(CH_3)_2$	0	NEt_2	Me	582	2.31	601	0.74	300	2.33×10^{-3}
52	$C(CH_3)_2$	1	H	Me	665	2.57	677	0.26	–	–
53	$C(CH_3)_2$	1	NEt_2	Me	668	2.33	686	0.52	42	1.64×10^{-2}
54	S	0	NEt_2	Et	594	–	606	0.40	1050	6.61×10^{-4}
55	S	1	NEt_2	Et	687	–	702	0.67	–	–
56	CH=CH	0	NEt_2	Bu	617	2.48	639	0.02	–	–
57	$C(CH_3)_2$	–	–	Me	585	–	608	0.55	7330	9.46×10^{-5}

Note: [a] half lifetime [75]; [b] hydrolytic rate constant

Table 10. Spectral properties of dyes bearing the BF_2-complex of 5-acetylbarbituric acid as the end-group

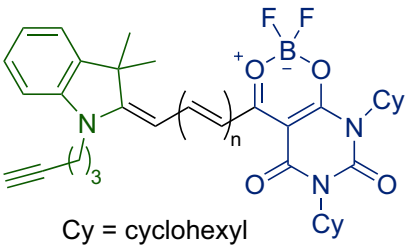

Cy = cyclohexyl

58, 60, 62

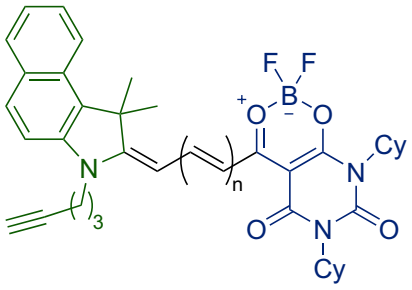

59, 61, 63

Dye	n	Solvent	λ^a_{max} [nm]	$\varepsilon \times 10^{-5}$ [M^{-1} cm^{-1}]	λ^f_{max} [nm]	Φ_f	$\varepsilon \times \Phi_f \times 10^{-5}$
58	1	toluene	528	0.94	550	0.3	0.28
		DMSO	540	0.77	558	0.37	0.29
59	1	toluene	551	1.24	572	0.68	0.84
		DMSO	563	1.10	583	0.18	0.20
60	2	toluene	615	2.03	642	0.35	0.71
		DMSO	644	3.63	665	0.42	1.52
61	2	toluene	634	1.68	661	0.65	1.09
		DMSO	663	2.41	687	0.26	0.63
62	3	toluene	683	1.09	727	0.21	0.23
		DMSO	748	2.31	779	0.33	0.76
63	3	toluene	705	0.89	746	0.18	0.16
		DMSO	770	1.83	794	0.18	0.33

2.4. Spectral properties of anionic dioxaborine-based polymethines

Spectral properties of anionic F_2DB-containing polymethines can be significantly altered by minor changes in both the structure of the end-groups and the length of the π-chain. For example, the insertion of $–CH_2–$ bridges into the end-groups of dye **64** via the *ortho*-position of the phenyl rings and position 5 of the F_2DB core induces a significant increase of the molar absorptivity (Table 11; ε(**65**)/ε(**64**) = 1.30) [83]. Compound **65** also intensely fluoresces at λ^f_{max} = 621 nm (Φ_f = 0.50 in DCM). However, when $–CH_2–CH_2–$ bridges are introduced, molar attenuation coefficients drop (ε(**66**)/ε(**64**) = 0.75), though its fluorescence intensity remains comparable to those of **65**.

Stiffening of the end-groups of dye **64** by –C(O)–O– bridges leads to a considerable increase

ISSN 2308-8303 (Print) / 2518-1548 (Online)

Table 11. Optical characteristics of anionic dioxaborine-containing polymethines in DCM

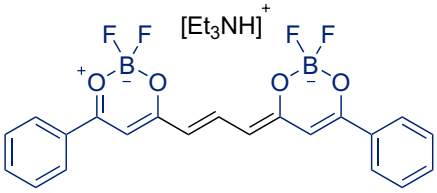

64

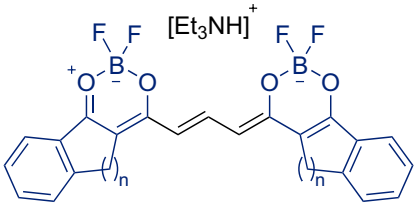

65: n = 1
66: n = 2

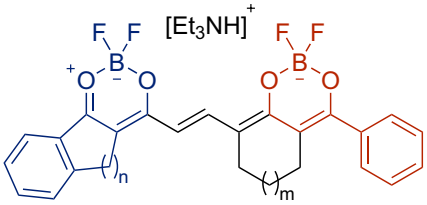

67: n = 1, m = 0
68: n = 2, m = 1

Compound	λ^{a}_{max} [nm]	$\varepsilon \times 10^{-5}$ [M^{-1} cm^{-1}]	λ^{f}_{max} [nm]	$\Delta\nu_s$ [cm^{-1}]	Φ_f
64	600	1.38	–	–	–
65	613	1.80	621	210	0.50
66	625	1.04	636	277	0.30
67	638	1.52	648	249	0.21
68	622	1.32	644	549	0.10

Table 12. Optical properties of symmetric anionic polymethines

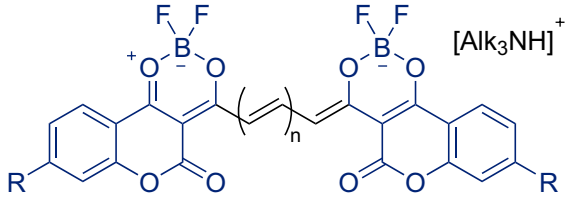

69, 70, 71-73

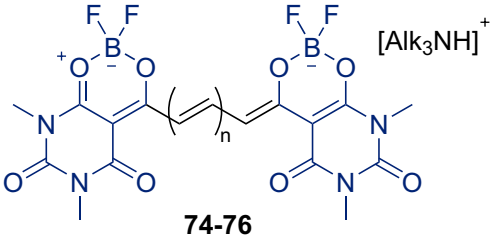

74-76

Compound	n	R	Alk	Solvent	λ^{a}_{max} [nm]	$\varepsilon \times 10^{-5}$ [M^{-1} cm^{-1}]	λ^{f}_{max} [nm]	$\Delta\nu_s$ [cm^{-1}]	Φ_f
69	1	H	Et	$CHCl_3$	581	2.11	588	205	0.19
				MeCN	572	2.15	581	271	0.04
70	1	NEt_2	*n*Bu	$CHCl_3$	625	2.36	635	252	0.85
				MeCN	615	2.52	639	611	0.4
71	2	H	Et	$CHCl_3$	678	2.13	687	193	
				MeCN	671	2.29	678	154	0.16
72	2	NEt_2	Et	$CHCl_3$	715	3.03	730	287	
				MeCN	712	3.00	732	384	0.76
73	3	NEt_2	Et	$CHCl_3$	817	–	–	–	–
				MeCN	810	2.86	–	–	–
74	1	–	Et	CH_2Cl_2	530	1.69	546	553	0.31
				MeCN	525	2.10	–	–	–
75	2	–	Et	CH_2Cl_2	630	2.03	651	512	0.82
				MeCN	625	2.22	–	–	–
76	3	–	Et	CH_2Cl_2	735	1.77	760	448	0.43
				MeCN	725	1.61	–	–	–

of the molar absorptivity (ε(**69**)/ε(**64**) = 1.53; Table 12) though its absorption maximum shifts hypsochromically by 19 nm in chlorinated solvents [78]. The insertion of a dialkylamino group into the *para*-position of the aromatic ring of the F_2DB end-group leads to an increase of the fluorescence quantum yield (Φ_f(**70**)/Φ_f(**69**) = 4.47 in $CHCl_3$). Lengthening of the polymethine chain of dye **70** by one vinylene group enhances the fluorescence intensity by almost two-fold in MeCN (**70** → **72**). Considering a high molar absorptivity of dye **72** (300000 M^{-1} cm^{-1} in MeCN), its brightness ($\varepsilon \times \Phi_f$) reaches the magnitude of 228000 M^{-1} cm^{-1}, which is outstandingly high for polymethine dyes, especially those emitting in the NIR region (λ^{f}_{max} = 732 nm for **72**). Similar to dyes **69**, **70**, and **71**–**73**, anionic polymethines **74**–**76** constructed from the BF_2-complex of 5-acetylbarbituric acid are also characterized by an intense absorption and a strong fluorescence [80].

Among the documented symmetric anionic dioxaborine-containing polymethines, the most deep-colored dyes are compounds **77** (λ^{a}_{max} = 844 nm in DCM) [80] and **78** (λ^{a}_{max} = 928 nm in DCM) [5]. Although these dyes are virtually non-fluorescent, their non-linear optical properties are

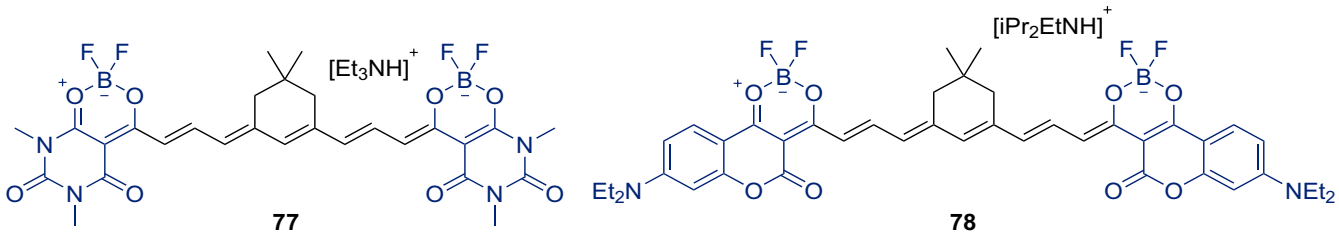

Figure 5. The long-chained symmetric anionic polymethines

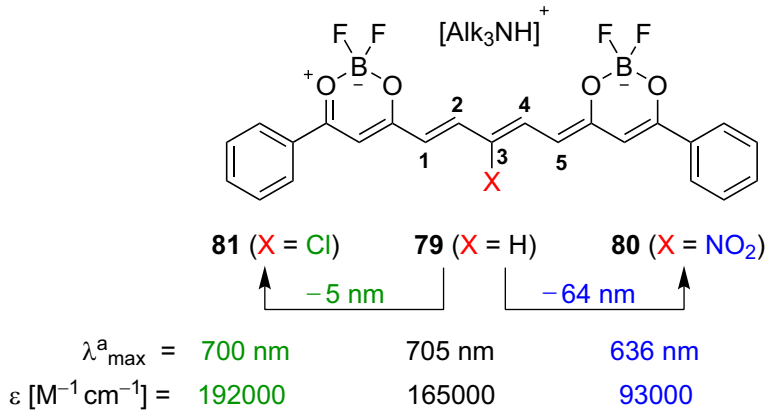

Figure 6. An example of alterations of the optical properties of the anionic dye through structural modifications of the π-chain (in DMSO)

more appealing [3, 6, 7]. For instance, the two-photon cross-section of compound **78** amounts to 17000 GM at 1100 nm in MeCN.

The vinylene shift of anionic polymethines is approximately 100 nm, which is similar to that of symmetric cationic dyes. The nature of a solvent (polar/non-polar, protic/aprotic) has a little effect on the positions of both absorption and emission maxima, while a small blueshift is observed when going from acetonitrile to DCM (or $CHCl_3$) [74, 78, 80]. Anionic F_2DB-containing polymethines are more resistant to the hydrolytic cleavage of the BF_2 group compared to F_2DB-containing merocyanines. Similar to merocyanines, the stability upon hydrolysis also increases when electron-donating functional groups are introduced into the aromatic ring of the F_2DB core [75].

Spectral properties of anionic polymethines can be significantly altered by the insertion of either electron-donating or electron-withdrawing substituents into the π-chain (Figure 6) [82]. For example, the replacement of H-atom at the *meso*-position of the pentamethine-bridged anionic dye by the NO_2 group (**79** → **80**) leads to a blueshift of the absorption maximum and a significant decrease of the absorption intensity (ε(**80**)/ε(**79**) = 0.56 in DMSO). These spectral changes agree with the Dewar-Knott color rules, according to which the electron-withdrawing substituents at odd-numbered positions of the π-chain induce a hypsochromic shift of the absorption maximum [89, 90].

The detailed investigation of the electronic structure of the anionic F_2DB-containing polymethines is reported elsewhere [80, 83, 91, 92]. In general, anionic dioxaborine-containing polymethines can be regarded as oxonol dyes, in which the negative charge is delocalized from the terminal O-atom of one end-group along the π-chain to the terminal O-atom of another end-group. A virtual build-up of the dioxaborine complex atop the heptamethine oxonol (**82** → **83**) results in a stabilization of HOMO (ΔE = 1.83 eV) and LUMO (ΔE = 0.85 eV) of the π-conjugated system [80, 93]. The long-wavelength absorption maximum of anionic polymethines is attributed to the $S_0 \rightarrow S_1$ electronic transition, while a less-intense higher energy shoulder ($\Delta\nu$ = 1200–1400 cm^{-1}) is attributed to the 0 → 1′ vibronic transition [92]. The BF_2-fragment is not involved in low-energy electronic transitions though it stabilizes significantly the anionic π-system.

3. Dyes with the dioxaborine ring in the polymethine chain

Dioxaborine can be regarded as integrated into the π-chain when the polymethine linkage is connected to positions 4 and 6 of the F_2DB core. When in such a framework the end-groups are electron donors, the overall electronic structure of the π-conjugated system attains a quadrupolar

ISSN 2308-8303 (Print) / 2518-1548 (Online)

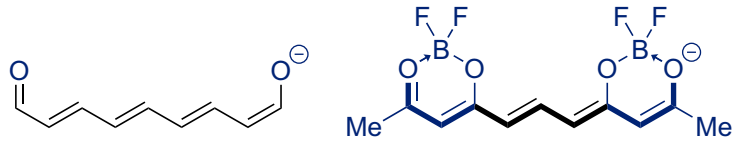

Figure 7. Structures of compounds **82** and **83**

character (the D–π–A–π–D type) [94]. In contrast to mesoionic cyanines built on the squarate or croconate core [95, 96], which also have a quadrupolar structure, the F_2DB-containing polymethines of the D–π–A–π–D type are characterized by the predominance of the neutral resonance form (without a charge separation) in the ground state.

The research on the F_2DB-containing quadrupolar merocyanines laid essentially dormant until 2009 when compounds **84** and **85** were discovered to have a strong fluorescent response upon binding to amyloid-β (Aβ) deposits [97] – a hallmark of Alzheimer's disease [98]. From this time on, both the diversity of the F_2DB-containing quadrupolar merocyanines and the range of their applications have been constantly growing.

3.1. Synthesis of BF_2-curcuminoids

Two general methods have been developed for the synthesis of dyes with the dioxaborine ring in the polymethine chain. The first one is the condensation of BF_2-acetylacetone with aromatic or cinnamic aldehydes [99] in the presence of either (i) base only (such as triethylamine [97], tetrahydroisoquinoline [68], or piperidine [100]) or (ii) base (often *n*-butylamine) with trialkyl borate as an additive [8, 101]. Trialkyl borate is shown to significantly increase the product yield though its mechanism of action has not been conclusively understood so far.

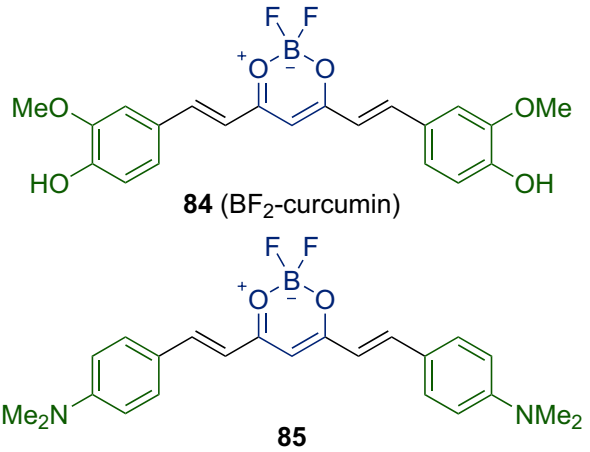

Figure 8. Structures of BF_2-curcumin and its analog **85**

The intermediate half-product can be isolated and put into the reaction with another aldehyde, thus yielding an asymmetric dye (Scheme 8) [68, 94, 99, 101].

The second method is a two-stage sequence with the initial construction of the β-diketonate-containing polymethine (curcumin-like scaffold or curcuminoid) followed by its treatment with BF_3 (Scheme 9) [102–105]. Acetylacetone (or its 5-alkyl- or 5-arylsubstituted derivative) reacts with boric anhydride producing the tetracoordinated boronic intermediate, which is further subjected into the reaction with aromatic aldehydes in the

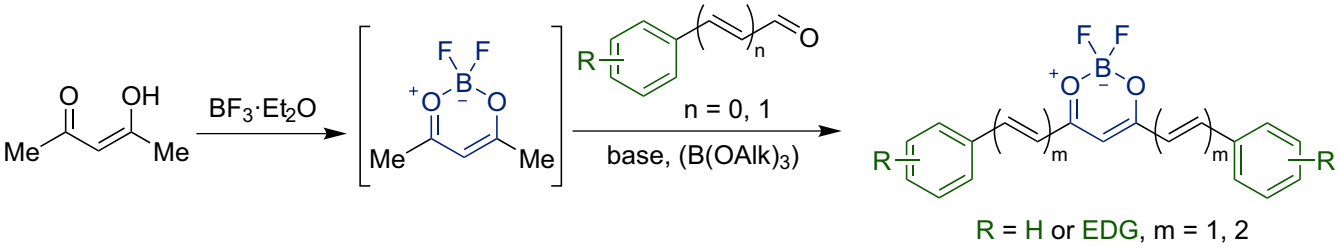

Scheme 7. The synthesis of symmetric BF_2-curcuminoids

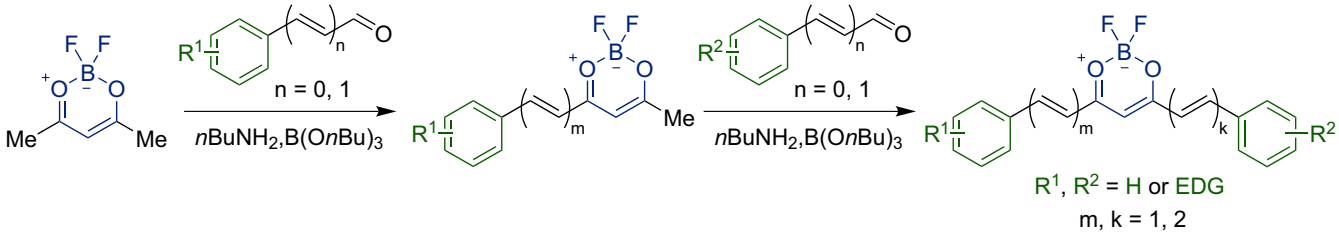

Scheme 8. The synthesis of asymmetric BF_2-curcuminoids

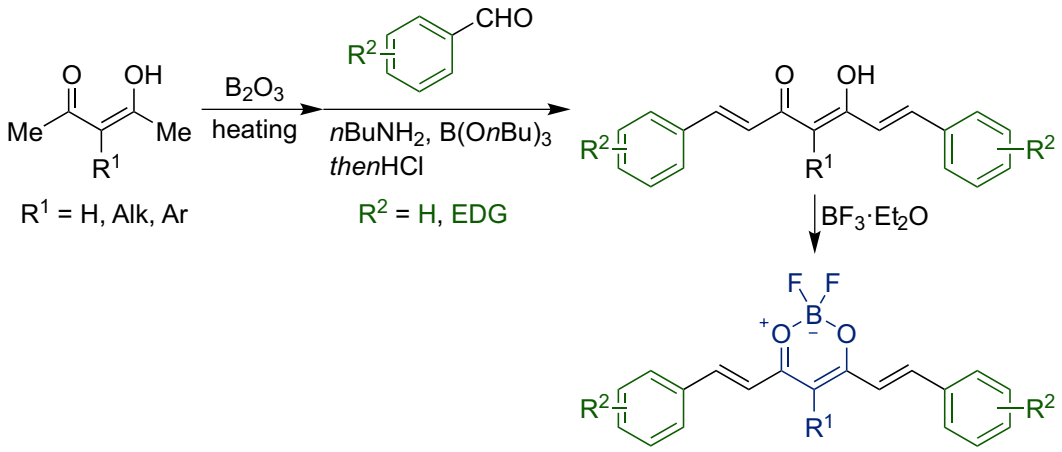

Scheme 9. An alternative route to symmetric BF_2-curcuminoids

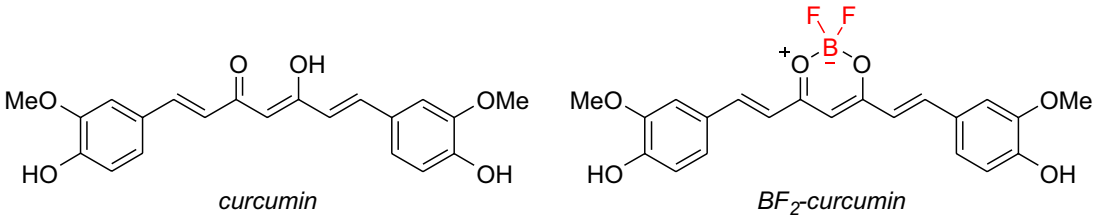

λ^a_{max} [nm]	λ^f_{max} [nm]	ε [$M^{-1}cm^{-1}$]	Φ_f	λ^a_{max} [nm]	λ^f_{max} [nm]	ε [$M^{-1}cm^{-1}$]	Φ_f
418	495	55000	0.10	**500**	**560**	**77000**	**0.34**

Figure 9. The influence of BF_2-chelation on spectral properties of curcumin

presence of *n*-butylamine and trialkyl borate. The product of this reaction is a tetracoordinated bis-curcuminoid, the acid-promoted decomposition of which results in a release of the curcuminoid scaffold. Then its treatment with $BF_3{\cdot}Et_2O$ fastens the *β*-diketonate backbone with the BF_2 group, forming the dioxaborine core.

3.2. Spectral characteristics

Basic spectral properties of the BF_2-curcuminoids are similar to those of dipolar F_2DB-merocyanines of type I: they absorb mostly in the visible range with the molar attenuation coefficients rarely exceeding 100000 M^{-1} cm^{-1}.

BF_2-chelated curcumin absorbs bathochromically by 82 nm (in DCM) and more intensely than the parent compound (Figure 9) [106]. The fluorescence quantum yield is also larger for the BF_2-derivative though the reported data on the Φ_f range of BF_2-curcumin is not conclusive. For example, paper [106] provides the Φ_f value of 0.34 in DCM, while earlier data from [107] give twice as large figure.

Similar to dipolar type I merocyanines, the position of λ^a_{max} is more sensitive to the structural modification of the end-groups than to the change of the π-chain length. For example, vinylene shifts of quadrupolar BF_2-merocyanines amount to approximately 50 nm depending on the end-groups (52 nm for **87** → **92**; 34 nm for **91** → **93**; Table 13) [100], while the replacement of H-atom by a dimethylamino group in the *para*-position of phenyl rings shifts the absorption maximum bathochromically by 150 nm (**87** → **85**). Note that the fluorescence intensity of **85** is nearly twice as large as that of **87**. The introduction of an electron-withdrawing cyano group at position 4 of phenyl rings shifts the long-wavelength λ^a_{max} hypsochromically by 26 nm with a little change of the fluorescence intensity [105].

BF_2-curcuminoids are positively solvatochromic, though the absorption maximum shift with an increase of the solvent polarity is not as large as for type I F_2DB-merocyanines [102]. However, in contrast to both dipolar and anionic dioxaborine-containing polymethines, quadrupolar BF_2-merocyanines are characterized by much more noticeable redshift of the emission maximum with the solvent polarity increase (Table 14). Moreover, the fluorochromic effect is larger for dyes bearing stronger electron-donating end-groups (compare $\Delta\upsilon_s$ values of **91** and **94**, Table 14).

The detailed investigation of the impact of both the electron donor strength of the end-groups and the nature of the solvent on spectral properties

ISSN 2308-8303 (Print) / 2518-1548 (Online)

Table 13. Spectral properties of BF_2-curcuminoids **86**–**93** in DCM

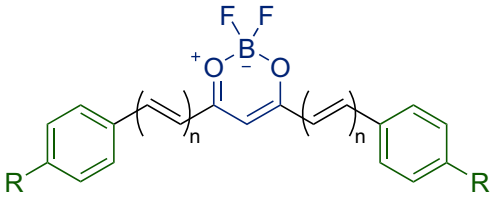

Dye	n	R	λ^a_{max} [nm]	$\varepsilon \times 10^{-5}$ [M^{-1} cm^{-1}]	λ^f_{max} [nm]	Φ_f	$\Delta\nu_s$ [cm^{-1}]
86	1	CN	421	0.59	–	0.19	–
87	1	H	447	0.45	484	0.24	1710
88	1	Me	464	0.56	–	0.15	–
89	1	Br	433	0.41	–	0.08	–
90	1	SMe	503	0.86	–	0.55	–
91	1	OMe	489	0.76	546	0.49	2130
85	1	NMe_2	597	0.45	681	0.47	2070
92	2	H	499	0.81	556	0.27	2050
93	2	OMe	523	0.83	625	0.24	3120

Table 14. Spectral properties of dyes **91** and **94** in solvents of different polarity

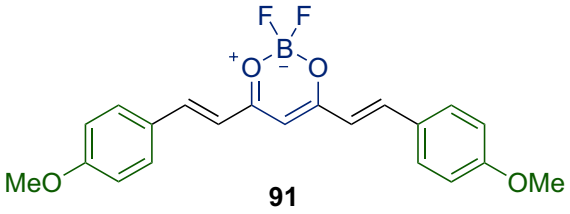

91

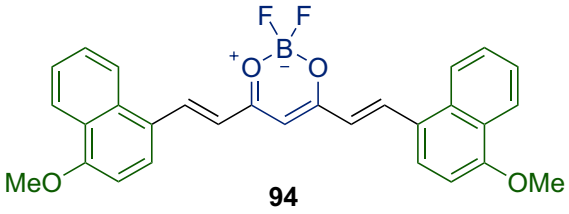

94

	91				**94**			
Solvent	λ^a_{max} [nm]	λ^f_{max} [nm]	Φ_f	$\Delta\nu_s$ [cm^{-1}]	λ^a_{max} [nm]	λ^f_{max} [nm]	Φ_f	$\Delta\nu_s$ [cm^{-1}]
CCl_4	477	492	0.20	640	523	561	0.23	1300
Et_2O	475	497	0.24	930	516	587	0.29	2340
AcOEt	480	515	0.35	1420	524	590	0.31	2140
DCM	488	538	0.44	1910	536	616	0.39	2420
acetone	483	534	0.45	1980	532	622	0.21	2720
MeCN	483	549	0.51	2490	530	651	0.12	3510

of BF_2-curcuminoids is reported elsewhere [94, 102, 108–111]. Generally, positive fluorochromism can be explained by higher energy requirement for the polar solvent to rearrange the solvate shell around the quadrupolar molecule during the relaxation from the Frank-Condon excited state S_1^{FC} to the relaxed state S_1 [102]. Since the excited state S_1 is more polar than the ground state S_0 and is characterized by the intramolecular charge transfer, enhancement of the electron donor power of the end-groups has an additional effect on the energy profile of relaxation $S_1^{FC} \rightarrow S_1$, which resulted in higher magnitudes of the Stokes shift [94, 102, 109].

3.3. Applications

The range of applications of BF_2-curcuminoids is varied broadly and predominantly relates to biochemical research. For example, besides dyes **84** and **85**, several other similar probes were developed for targeting amyloid-β aggregates. These include dye **95**, which was specifically designed to target soluble forms of Aβ [68], allowing detection of the early stages of the disease, when symptoms had not yet become apparent. Bifunctional probe **96** is proved effective for both targeting the Aβ deposits and inhibition of the metal-catalyzed cross-coupling of Aβ [112]. The latter ability greatly diminishes the speed of formation of insoluble forms of Aβ plaques, thus slowing down the disease progression. Probe **97** capable of detecting both soluble and insoluble Aβ species by applying the near-infrared fluorescence (NIRF) molecular imaging [113]. It was the first time when the NIRF technique was demonstrated to be effectively used for the therapy of Alzheimer's disease.

The mechanism of action of compounds **95**–**97** is based on non-covalent interaction between the probe and a biomolecule. The BF_2-curcuminoid scaffold is also suitable for designing probes for

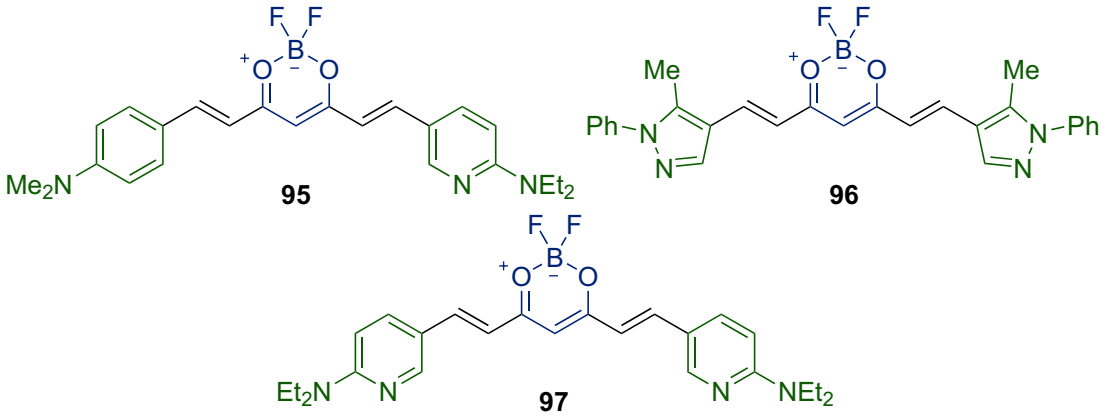

Figure 10. Fluorogenic probes for the therapy of Alzheimer's disease

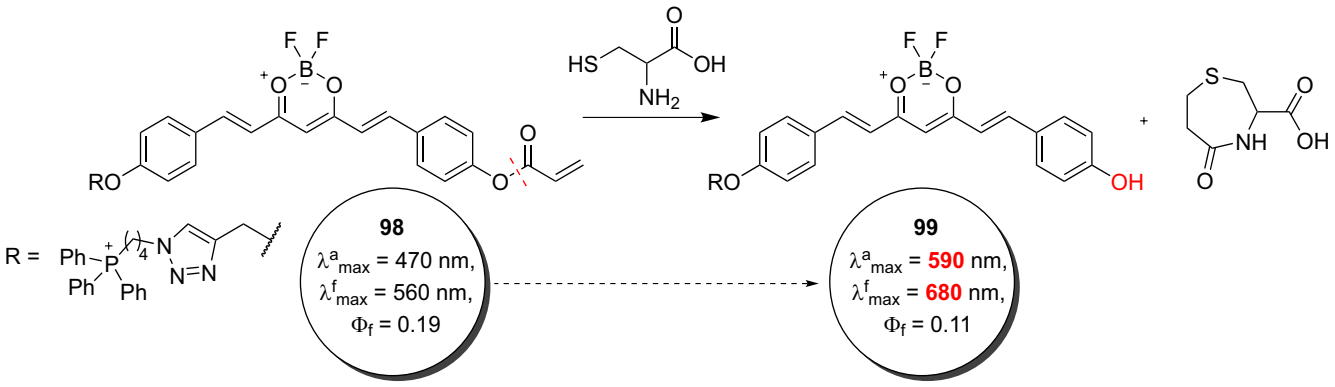

Scheme 10. Ratiometric detection of cysteine using probe **98**

specific covalent targeting where functionalized electron donor end-groups serve as active sites. The illustrative example is compound **98**, which was developed for detecting mitochondrial cysteine (Cys) [114]. The acrylic ester active site of probe **98** cleaves upon the presence of cysteine, thus ratiometrically detecting the biothiol.

Besides cysteine, homocysteine (Hcy) and glutathione (GSH) can be targeted using fluorogenic probe **100** [115]. Upon the interaction with biothiols the 2.4-(dinitrobenzene)sulfonate active groups are cleaved releasing BF_2-curcumin. The process is accompanied by an increase of the fluorescence intensity at 610 nm.

For targeting of γ-glutamyl transpeptidase (GGT) – a biomarker, the accumulation of which is connected with progression of several types of cancer – the fluorogenic probe **101** was designed [116]. The cleavage of the glutamyl substituent of compound **101** in the presence of GGT is accompanied by a strong fluorescence response in the far-visible region.

In addition to biomedical research, BF_2-curcuminoids were also examined for applications in photovoltaics. For example, compounds **103**–**105** were utilized as donor materials in solution-processed bulk-heterojunction organic solar cells (BHJ OSCs) by blending with acceptor [6,6]-phenyl-C_{61}-butyric acid methyl ester [117]. The result-

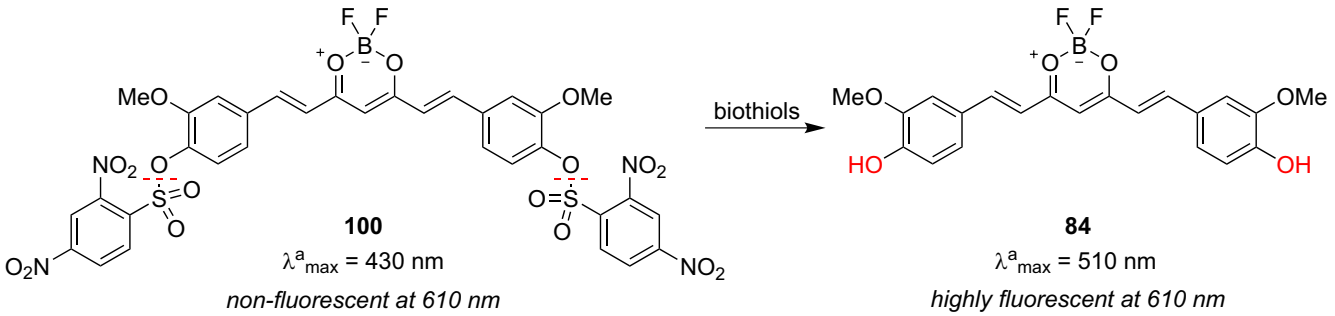

Scheme 11. Application of probe **100** for detection of biothiols

ISSN 2308-8303 (Print) / 2518-1548 (Online)

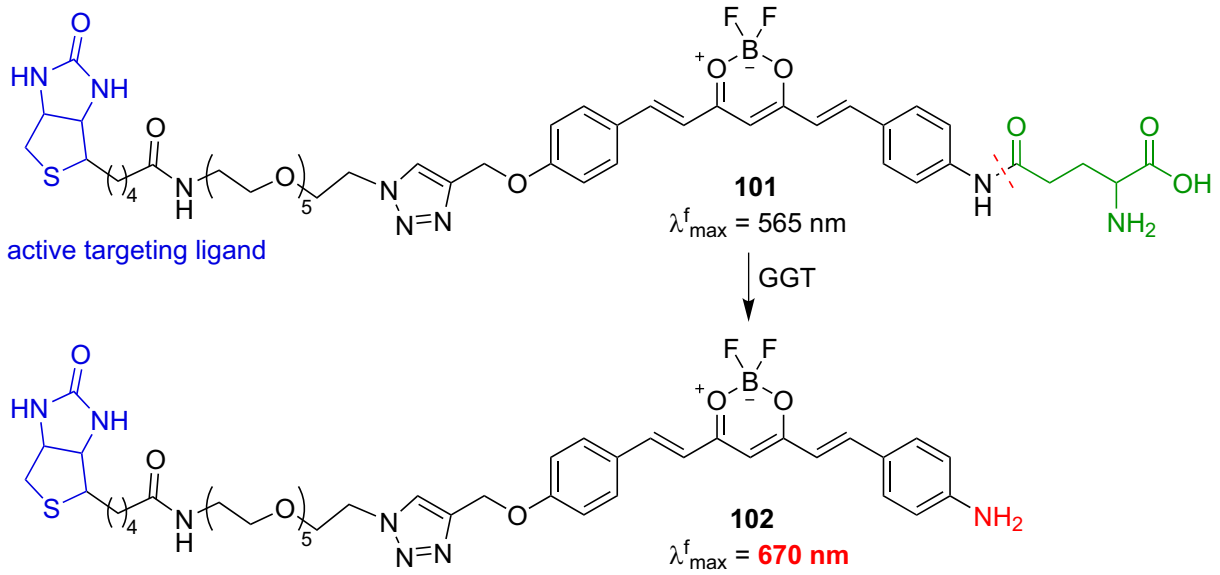

Scheme 12. Targeting of GGT using a selective fluorogenic probe **101**

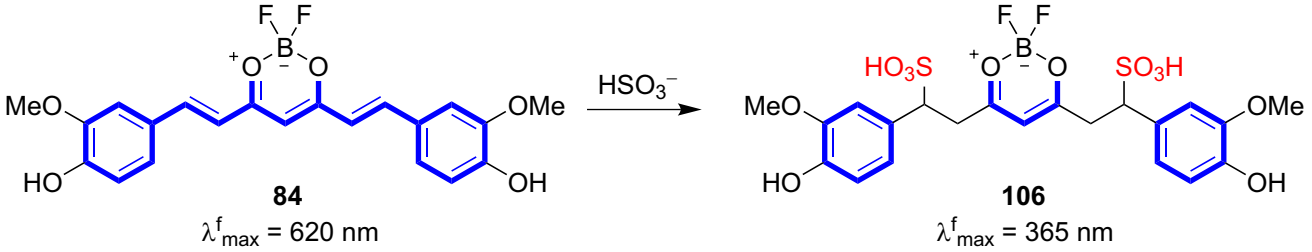

Scheme 13. Detection of a bisulfite ion with curcumin

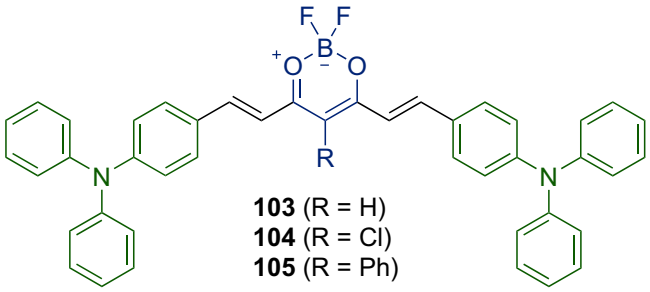

Figure 11. BF_2-curcuminoids used in photovoltaics

ing photoelements displayed the power conversion efficiency up to 4.14%, thus showing potential of quadrupolar BF_2-merocyanines for fabrication of BHJ OSCs.

The very BF_2-curcumin was shown to be highly sensitive to the presence of a cyanide ion [107, 118]. The interaction of CN^- with BF_2-curcumin leads to a considerable redshift of the absorption maximum (from 507 nm to 649 nm) with concomitant quenching of the fluorescence emission. These spectral effects are caused by deprotonation of hydroxy substituents of the end-groups yielding the dianion (in non-aqueous media), which have no detectable emission due to the photoinduced charge transfer from the negatively charged end-groups to the dioxaborine core.

Besides cyanide, bisulfite ion can be also detected by BF_2-curcumin [119] though in this case the sensory mechanism is different. HSO_3^- acts as a Michael donor attacking the double bonds of the π-chain and forming adduct **106** (Scheme 13). As a result, the π-conjugated system of the dye becomes fragmented and the peak at 620 nm disappears.

4. *Meso*-cyano-substituted dioxaborine – a new building block for the brightest polymethines

Despite a broad range of applications, quadrupolar dioxaborine-containing merocyanines were only represented by BF_2-curcuminoids not so long ago. While there is a vast diversity of dipolar F_2DB-merocynines with weak (type I) and strong (type II) electron-donor end-groups until recently there was only one quadrupolar F_2DB-merocyanine constituting strong electron-donor end-groups [120]. With the advent of the BF_2-complex of *meso*-cyano acetylacetone the diversity of such compounds has become greatly enriched (Figure 12). Moreover, the exploration of chemical properties of **107** yielded new types of polymethine dyes, such as mero-anionic and polyanionic polymethines possessing outstanding spectral properties.

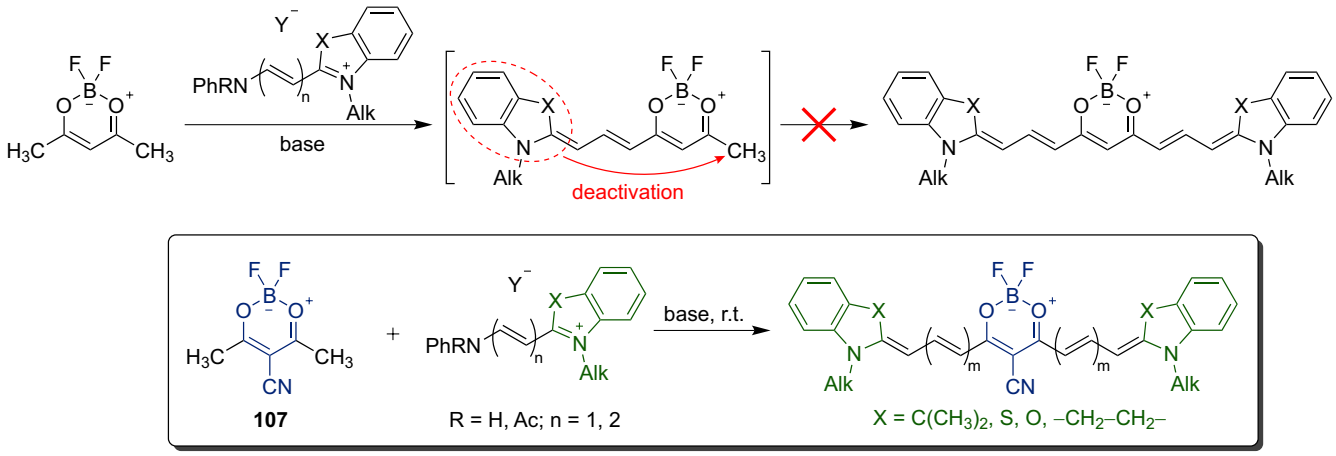

Scheme 14. The synthesis of quadrupolar merocyanines from *meso*-cyano-substituted dioxaborine

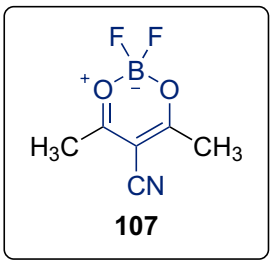

Figure 12. The BF_2-complex of *meso*-cyano acetylacetone

4.1. Quadrupolar merocyanines and mero-anionic dyes

The key feature of the cyano-substituted BF_2-acetylacetone is higher acidity of its methyl groups compared to the parent compound **2**, thus making substrate **107** more active towards electrophiles. Thus, while the reaction of BF_2-acetylacetone with cationic hemicyanines often results in mono-condensation, since the activity of the second methyl group gets too low for the reaction to proceed further, bis-condensation products are easily obtained by the reaction of **107** with hemicyanines even at room temperature (Scheme 14) [121].

A high activity of the methyl group of the half-product (i. e., the product of the mono-condensation of **107** with hemicyanines) allows carrying out chemical transformations with other electrophiles. For example, the reaction of such half-products with ethoxymethylene or 2-anilinovinyl derivatives of CH-acids in the presence of a base, such as triethylamine or diisopropylethylamine, and acetic anhydride results in the formation of polymethines of the unusual D–π–A–π–A′ type (Scheme 15). Since these compounds comprise the dipolar merocyanine (D–π–A) and non-symmetric anionic (A–π–A′) parts in their scaffold, the dubbing "mero-anionic" dyes was introduced for distinguishing them from other types of polymethines [122].

The tendencies in alterations of spectral properties upon the transition from BF_2-curcuminoids to quadrupolar merocyanines with heterocyclic

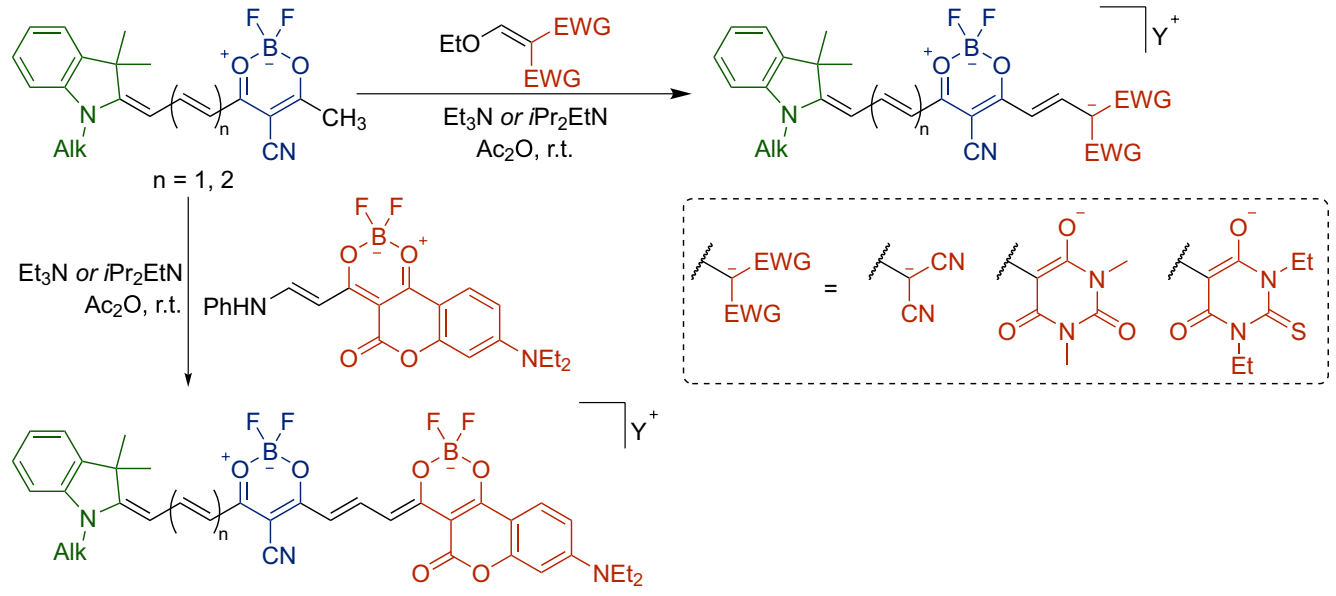

Scheme 15. The synthesis of mero-anionic polymethines

ISSN 2308-8303 (Print) / 2518-1548 (Online)

Table 15. Spectral properties of quadrupolar cyanodioxaborine-containing polymethines in DCM

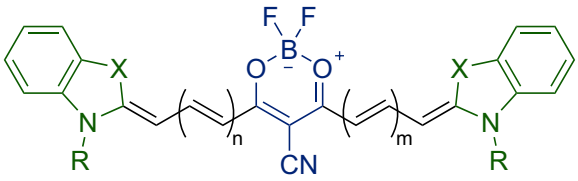

Dye	X	R	n	m	λ^{a}_{max} [nm]	$\varepsilon \times 10^{-4}$ [M^{-1} cm^{-1}]	λ^{f}_{max} [nm]	Φ_f
108	$C(CH_3)_2$	CH_3	1	1	667	2.75	702	0.72
109	S	$C_{10}H_{21}$	1	1	702	2.89	730	0.68
110	$C(CH_3)_2$	CH_3	1	2	740	2.42	792	0.45
111	$C(CH_3)_2$	CH_3	2	2	808	2.59	880	0.07

Table 16. UV-Vis spectral characteristics of mero-anionic dyes

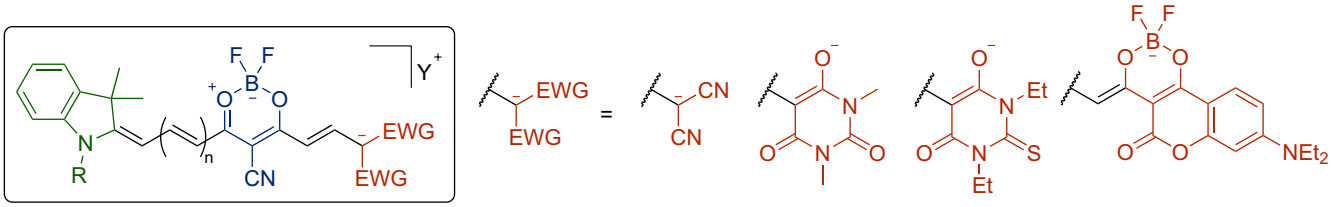

112, 116 **113, 117** **114, 118** **115, 119**

Dye	R	n	Y^+	Solvent	λ_a [nm]	$\varepsilon \times 10^{-5}$ [M^{-1} cm^{-1}]	λ_f [nm]	Φ_f	$\varepsilon \times \Phi_f \times 10^{-5}$ [M^{-1} cm^{-1}]
112	CH_3	1	$[Et_4N]^+$	DCM	598	0.86	629	0.20	0.17
				DMF	605	1.59	634	0.61	0.97
113	CH_3	1	$[Et_3NH]^+$	DCM	621	2.18	652	0.84	1.83
				DMF	623	2.09	651	0.64	1.34
114	CH_3	1	$[Et_3NH]^+$	DCM	634	2.33	664	0.83	1.92
				DMF	638	2.52	663	0.80	2.02
115	CH_3	1	$[Et_3NH]^+$	DCM	706	2.86	729	0.50	1.42
				DMF	706	3.37	733	0.52	1.30
116	*n*Pr	2	$[Et_3NH]^+$	DCM	670	1.19	724	0.19	0.22
				DMF	675	1.20	729	0.37	0.44
117	*n*Bu	2	$[iPr_2EtNH]^+$	DCM	697	1.59	743	0.32	0.51
				DMF	694	1.47	743	0.32	0.46
118	*n*Bu	2	$[iPr_2EtNH]^+$	DCM	710	1.79	757	0.41	0.74
				DMF	716	2.08	759	0.49	1.02
119	*n*Pr	2	$[Et_3NH]^+$	DCM	776	2.61	813	0.20	0.53
				DMF	777	3.03	823	0.060	0.18

end-groups is similar to those of the transition from type I to type II dipolar F_2DB-merocyanines (see Sect 3.3.). For example, the quadrupolar merocyanines absorb and emit mostly in the NIR spectral range (Table 15) [121]. While molar absorptivities of BF_2-curcuminoids are usually below 100000 M^{-1} cm^{-1}, the D–π–A–π–D type F_2DB-containing polymethines have the attenuation coefficients of 250000 M^{-1} cm^{-1} and above. Their fluorescence quantum yields also tend to be higher, reaching, for example, 0.72 and 0.68 in DCM for polymethines with indolenine and benzothiazole end-groups (**108** and **109**), respectively. Vinylene shifts are also higher than in BF_2-curcuminoids, equaling 73 nm for **108** → **110** and 68 nm for **110** → **111**.

Mero-anionic dyes are also characterized by an intense absorption and a strong fluorescence in far-visible and NIR regions (Table 16) [122]. The distinctive feature of mero-anionic dyes is a broad range of modulation of optical properties by tuning the structure of the accepting end-group. For example, dyes with the malononitrile end-group (**112** and **116**) are characterized by relatively low molar attenuation coefficients, while the molar absorptivity of dyes **115** and **119** bearing the coumarino-dioxaborine end-group reaches 300000 M^{-1} cm^{-1}. The vinylene shift is in a range of 60–80 nm depending on the structure of the end-groups.

4.2. Polyanionic polymethines

Synthetic possibilities of *meso*-cyano-substituted dioxaborine **107** go beyond synthesis of

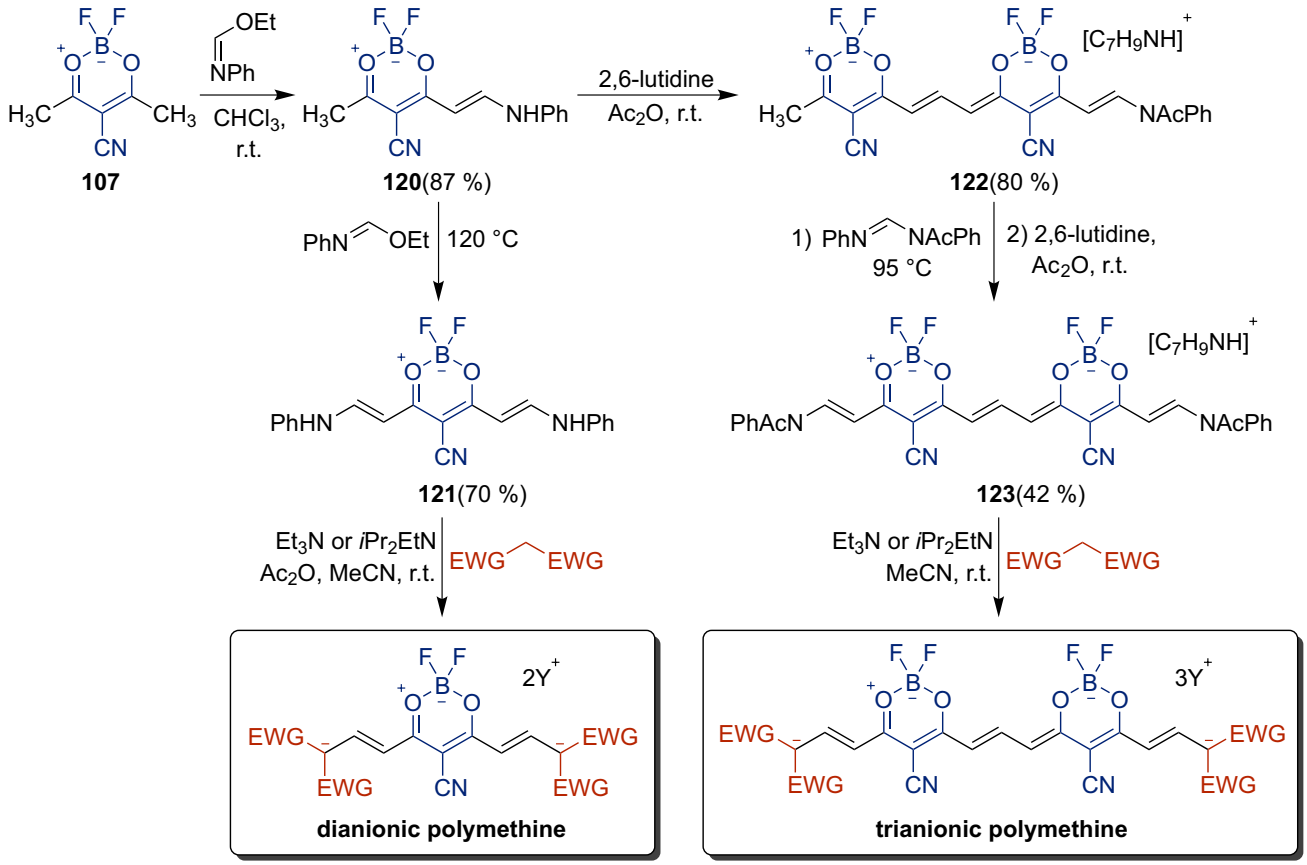

Scheme 16. The synthesis of dianionic and trianionic dyes

Table 17. Spectral properties of polyanionic dyes in DMF

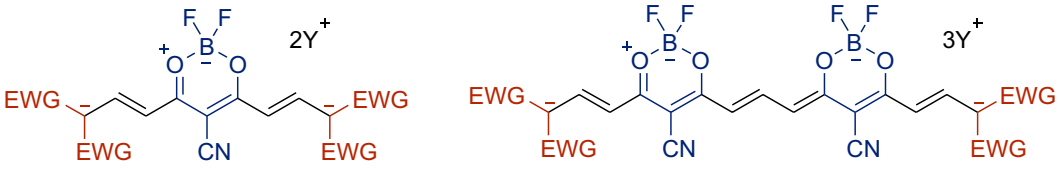

124-127 **128-131**

Dye	End-group	Y+	λ^{a}_{max} [nm]	$\varepsilon \times 10^{-5}$ [M^{-1} cm^{-1}]	λ^{f}_{max} [nm]	Φ_f	$\varepsilon \times \Phi_f \times 10^{-5}$ [M^{-1} cm^{-1}]
Dianionic polymethines							
124	malononitrile	$[Et_4N]^+$	538	2.38	553	0.90	2.14
125	1,3-dimethylbarbituric acid	$[Et_3NH]^+$	570	2.53	586	0.92	2.33
126	1,3-diethylthiobarbituric acid	$[Et_3NH]^+$	597	2.93	614	0.87	2.55
127	1,3-indandione	$[iPr_2EtNH]^+$	624	3.26	640	0.61	1.99
Trianionic polymethines							
128	malononitrile	$[nBu_4N]^+$	687	4.29	705	0.73	3.13
129	1,3-dimethylbarbituric acid	$[nBu_4N]^+$	705	4.21	725	0.64	2.69
130	1,3-diethylthiobarbituric acid	$[nBu_4N]^+$	722	4.32	741	0.49	2.12
131	1,3-indandione	$[nBu_4N]^+$	751	4.95	770	0.50	2.48

quadrupolar merocyanines and mero-anionic dyes. Recently, the first representatives of dianionic [123] and trianionic [124] polymethines were synthesized (Scheme 16). For the synthesis of dianionic polymethines, the intermediate bis-hemicyanine **121** was obtained, while bis-hemicyanine **123**, a precursor to trianionic dyes, was obtained in several steps from compound **120**. Subjecting compounds **121** and **123** into reactions with CH-acids (malononitrile, 1,3-indandione, barbituric and thiobarbituric acids) yields the corresponding dianionic and trianionic polymethines.

Dianionic and trianionic dioxaborine-containing polymethines are strongly emissive, with the fluorescence quantum yield reaching 0.90 for dianionic and 0.73 for trianionic dyes in DMF (Table 17). While dianionic dyes fluoresce in the far-visible region, trianionic dyes emit in the NIR

ISSN 2308-8303 (Print) / 2518-1548 (Online)

region, thus becoming the brightest reported NIR-emitters among the polymethine dyes. Moreover, trianionic dyes are characterized by a remarkably high molar attenuation coefficients, reaching, for example, 495000 M^{-1} cm^{-1} for dye **131** in DMF. The fluorescence brightness of polyanionic dioxaborine dyes is also unmatched among polymethines, reaching or exceeding the value of 250000 M^{-1} cm^{-1} in DMF.

Conclusions

Modern organic chemistry is driven by a rising demand for high-performance materials for applications in both existing and emerging technologies. Dioxaborine-containing π-conjugated systems are a good example of versatile functional compounds that combine high synthetic potential and flexibility in molecular modelling. As was outlined in the present Perspective, these features allow creating highly effective solutions based on the F_2DB-containing dyes for various kinds of photoenergy-transformation domains, ranging from biomedical research to non-linear optics. With scores of new publications each year, the contribution of dioxaborine-containing compounds to the development of a new generation of materials possessing specific physicochemical properties has been constantly growing. An illustrative example is the recently reported synthesis of highly fluorescent polyanionic dyes, which exposed vast potential of the F_2DB core for obtaining bright NIR fluorophores. Further research may revolve around the synthesis of water-soluble dioxaborine-containing polymethines, which makes them highly attractive probes for medicinal application. Overcoming the intrinsic instability in relation to acidic and basic solvolysis is another promising path for further investigations. We believe that this review will serve as a useful guide in navigating a vast body of research dedicated to diverse types of dioxaborine-containing polymethines, kindling thus an additional interest for future studies.

References

1. Mishra, A.; Behera, R. K.; Behera, P. K.; Mishra, B. K.; Behera, G. B. Cyanines during the 1990s: A Review. *Chem. Rev.* **2000**, *100* (6), 1973–2012. https://doi.org/10.1021/cr990402t.
2. Kammler, R.; Bourhill, G.; Jin, Y.; Bräuchle, C.; Görlitz, G.; Hartmann, H. Second-Order Optical Non-Linearity of New 1,3,2(2H)-Dioxaborine Dyes. *J. Chem. Soc., Faraday Trans.* **1996**, *92* (6), 945–947. https://doi.org/10.1039/FT9969200945.
3. Hales, J. M.; Zheng, S.; Barlow, S.; Marder, S. R.; Perry, J. W. Bisdioxaborine Polymethines with Large Third-Order Nonlinearities for All-Optical Signal Processing. *J. Am. Chem. Soc.* **2006**, *128* (35), 11362–11363. https://doi.org/10.1021/ja063535m.
4. Padilha, L. A.; Webster, S.; Przhonska, O. V.; Hu, H.; Peceli, D.; Rosch, J. L.; Bondar, M. V.; Gerasov, A. O.; Kovtun, Y. P.; Shandura, M. P.; Kachkovski, A. D.; Hagan, D. J.; Van Stryland, E. W. Nonlinear Absorption in a Series of Donor–π–Acceptor Cyanines with Different Conjugation Lengths. *J. Mater. Chem.* **2009**, *19* (40), 7503. https://doi.org/10.1039/b907344b.
5. Padilha, L. A.; Webster, S.; Przhonska, O. V.; Hu, H.; Peceli, D.; Ensley, T. R.; Bondar, M. V.; Gerasov, A. O.; Kovtun, Y. P.; Shandura, M. P.; Kachkovski, A. D.; Hagan, D. J.; Stryland, E. W. Van. Efficient Two-Photon Absorbing Acceptor-π-Acceptor Polymethine Dyes. *J. Phys. Chem. A* **2010**, *114* (23), 6493–6501. https://doi.org/10.1021/jp100963e.
6. Matichak, J. D.; Hales, J. M.; Ohira, S.; Barlow, S.; Jang, S.-H.; Jen, A. K.-Y.; Brédas, J.-L.; Perry, J. W.; Marder, S. R. Using End Groups to Tune the Linear and Nonlinear Optical Properties of Bis(Dioxaborine)-Terminated Polymethine Dyes. *ChemPhysChem* **2010**, *11* (1), 130–138. https://doi.org/10.1002/cphc.200900635.
7. Lin, H.-C.; Kim, H.; Barlow, S.; Hales, J. M.; Perry, J. W.; Marder, S. R. Synthesis and Linear and Nonlinear Optical Properties of Metal-Terminated Bis(Dioxaborine) Polymethines. *Chem. Commun.* **2011**, *47* (2), 782–784. https://doi.org/10.1039/C0CC02003F.
8. Pitter, D. R. G.; Brown, A. S.; Baker, J. D.; Wilson, J. N. One Probe, Two-Channel Imaging of Nuclear and Cytosolic Compartments with Orange and Red Emissive Dyes. *Org. Biomol. Chem.* **2015**, *13* (36), 9477–9484. https://doi.org/10.1039/C5OB01428J.
9. Collot, M.; Fam, T. K.; Ashokkumar, P.; Faklaris, O.; Galli, T.; Danglot, L.; Klymchenko, A. S. Ultrabright and Fluorogenic Probes for Multicolor Imaging and Tracking of Lipid Droplets in Cells and Tissues. *J. Am. Chem. Soc.* **2018**, *140* (16), 5401–5411. https://doi.org/10.1021/jacs.7b12817.
10. Ashoka, A. H.; Ashokkumar, P.; Kovtun, Y. P.; Klymchenko, A. S. Solvatochromic Near-Infrared Probe for Polarity Mapping of Biomembranes and Lipid Droplets in Cells under Stress. *J. Phys. Chem. Lett.* **2019**, *10* (10), 2414–2421. https://doi.org/10.1021/acs.jpclett.9b00668.
11. Gerasov, A.; Shandura, M.; Kovtun, Y.; Losytskyy, M.; Negrutska, V.; Dubey, I. Fluorescent Labeling of Proteins with Amine-Specific 1,3,2-(2H)-Dioxaborine Polymethine Dye. *Anal. Biochem.* **2012**, *420* (2), 115–120. https://doi.org/10.1016/j.ab.2011.09.018.
12. Sun, Q.; Wang, W.; Chen, Z.; Yao, Y.; Zhang, W.; Duan, L.; Qian, J. A Fluorescence Turn-on Probe for Human (Bovine) Serum Albumin Based on the Hydrolysis of a Dioxaborine Group Promoted by Proteins. *Chem. Commun.* **2017**, *53* (48), 6432–6435. https://doi.org/10.1039/C7CC03587J.
13. Li, Z.; Wang, Y.; Li, M.; Chen, H.; Xie, Y.; Li, P.; Guo, H.; Ya, H. Solvent-Dependent and Visible Light-Activated NIR Photochromic Dithienylethene Modified by Difluoroboron β-Diketonates as Fluorescent Turn-on PH Sensor. *Dyes Pigm.* **2019**, *162*, 339–347. https://doi.org/10.1016/j.dyepig.2018.10.049.
14. Karpenko, I. A.; Niko, Y.; Yakubovskyi, V. P.; Gerasov, A. O.; Bonnet, D.; Kovtun, Y. P.; Klymchenko, A. S. Push–Pull Dioxaborine as Fluorescent Molecular Rotor: Far-Red Fluorogenic Probe for Ligand–Receptor Interactions. *J. Mater. Chem. C* **2016**, *4* (14), 3002–3009. https://doi.org/10.1039/C5TC03411F.
15. Han, W.; You, J.; Li, H.; Zhao, D.; Nie, J.; Wang, T. Curcuminoid-Based Difluoroboron Dyes as High-Performance Photosensitizers in Long-Wavelength (Yellow and Red) Cationic Photopolymerization. *Macromol. Rapid Commun.* **2019**, *40* (20), 1900291. https://doi.org/10.1002/marc.201900291.

16. Zhou, Y.; Chen, Y.-Z.; Cao, J.-H.; Yang, Q.-Z.; Wu, L.-Z.; Tung, C.-H.; Wu, D.-Y. Dicyanoboron Diketonate Dyes: Synthesis, Photophysical Properties and Bioimaging. *Dyes Pigm.* **2015**, *112*, 162–169. https://doi.org/10.1016/j.dyepig.2014.07.001.
17. Cheng, X.; Li, D.; Zhang, Z.; Zhang, H.; Wang, Y. Organoboron Compounds with Morphology-Dependent NIR Emissions and Dual-Channel Fluorescent ON/OFF Switching. *Org. Lett.* **2014**, *16* (3), 880–883. https://doi.org/10.1021/ol403639n.
18. Chen, P.-Z.; Niu, L.-Y.; Chen, Y.-Z.; Yang, Q.-Z. Difluoroboron β-Diketonate Dyes: Spectroscopic Properties and Applications. *Coord. Chem. Rev.* **2017**, *350*, 196–216. https://doi.org/10.1016/j.ccr.2017.06.026.
19. Collot, M. Recent Advances in Dioxaborine-Bxased Fluorescent Materials for Bioimaging Applications. *Mater. Horiz.* **2021**, *8* (2), 501–514. https://doi.org/10.1039/D0MH01186J.
20. Delgado, D.; Abonia, R. Synthetic Approaches for BF2-Containing Adducts of Outstanding Biological Potential. A Review. *Arabian J. Chem.* **2022**, *15* (1), 103528. https://doi.org/10.1016/j.arabjc.2021.103528.
21. Vanallan, J. A.; Reynolds, G. A. The Reactions of 2,2-Difluoro-4-Methylnaphtho[l,2-e]-1,3,2-Dioxaborin and Its [2,1-e] Isomer with Carbonyl Compounds and with Aniline. *J. Heterocycl. Chem.* **1969**, *6* (1), 29–35. https://doi.org/10.1002/jhet.5570060106.
22. Dilthey, W.; Eduardoff, F.; Schumacher, F. J. Ueber Siliconium-, Boronium- Und Titanoniumsalze. Zum Theil Gemeinschaftlich Mit. *Justus Liebigs Ann. Chem.* **1906**, *344* (3), 300–313. https://doi.org/10.1002/jlac.19063440305.
23. Morgan, G. T.; Tunstall, R. B. CCLIII.—Researches on Residual Affinity and Coordination. Part XXI. Boron β-Diketone Difluorides. *J. Chem. Soc., Trans.* **1924**, *125*, 1963–1967. https://doi.org/10.1039/CT9242501963.
24. Shokova, E. A.; Kim, J. K.; Kovalev, V. V. evich. 1,3-Diketones. Synthesis and Properties. *Russ. J. Org. Chem.* **2015**, *51* (6), 755–830. https://doi.org/10.1134/S1070428015060019.
25. Kel'in, A. Recent Advances in the Synthesis of 1,3-Diketones. *Curr. Org. Chem.* **2003**, *7* (16), 1691–1711. https://doi.org/10.2174/1385272033486233.
26. Young, F. G.; Frostick, F. C.; Sanderson, J. J.; Hauser, C. R. Conversion of Ketone Enol Esters to β-Diketones by Intramolecular Thermal Rearrangement and by Intermolecular Acylations Using Boron Fluoride. *J. Am. Chem. Soc.* **1950**, *72* (8), 3635–3642. https://doi.org/10.1021/ja01164a088.
27. Meerwein, H.; Vossen, D. Synthesen von Ketonen Und β-Diketonen Mit Hilfe von Borfluorid. *Journal für Praktische Chemie* **1934**, *141* (5–8), 149–166. https://doi.org/10.1002/PRAC.19341410503.
28. Hauser, C. R.; Frostick, F. C.; Man, E. H. Mechanism of Acetylation of Ketone Enol Acetates with Acetic Anhydride by Boron Trifluoride to Form β-Diketones. *J. Am. Chem. Soc.* **1952**, *74* (13), 3231–3233. https://doi.org/10.1021/ja01133a008.
29. Youssefyeh, R. D. Acylations of Ketals and Enol Ethers. *J. Am. Chem. Soc.* **1963**, *85* (23), 3901–3902. https://doi.org/10.1021/ja00906a047.
30. Durden, J. A.; Crosby, D. G. The Boron Trifluoride Catalyzed Reaction of Acetophenone with Acetic Anhydride. *J. Org. Chem.* **1965**, *30* (5), 1684–1687. https://doi.org/10.1021/jo01016a527.
31. Schiemenz, G. P.; Schmidt, U. Trimethoxyphenylverbindungen, IX. Borheterocyclen in Der Präparativen Naturstoffchemie: Eine Einfache Synthese Des Aurentiacins. *Liebigs Annalen der Chemie* **1982**, *1982* (8), 1509–1513. https://doi.org/10.1002/JLAC.198219820810.
32. Czerney, P.; Igney, C.; Haucke, G.; Hartmann, H. Zur Synthese Und Spektralen Charakterisierung von Verbrückten 2, 2-Difluoro-1,3,2-Dioxaborinen. *Zeitschrift für Chemie* **1988**, *28* (1), 23–24. https://doi.org/10.1002/ZFCH.19880280105.
33. Görlitz, G.; Hartmann, H. On the Formation and Solvolysis of 4-Aryl-2,2-Difluoro-6-Methyl-1,3,2-(2H)-Dioxaborines. *Heteroat. Chem.* **1997**, *8* (2), 147–155. https://doi.org/10.1002/(SICI)1098-1071(1997)8:2<147::AID-HC7>3.0.CO;2-B.
34. Görlitz, G.; Hartmann, H.; Nuber, B.; Wolff, J. J. A Simple Route to 4-Aryl and 4-Hetaryl Substituted 6-Methyl-2,2-Difluoro-1,3,2-(2H)-Dioxaborines. *Journal für praktische Chemie* **1999**, *341* (2), 167–172. https://doi.org/10.1002/(SICI)1521-3897(199902)341:2<167::AID-PRAC167>3.0.CO;2-A.
35. Hauser, C. R.; Eby, C. J. The Conversion of β-Ketonitriles to β-Ketoamides by Boron Fluoride in Aqueous Acetic Acid and by Polyphosphoric Acid 1. *J. Am. Chem. Soc.* **1957**, *79* (3), 725–727. https://doi.org/10.1021/ja01560a061.
36. Hartmann H.; Hunze A.; Kanitz A.; Rogler W.; Rohde D. Amorphous organic 1,3,2-dioxaborine luminophores method for the production and use thereof. U. S. Patent US20040065867A1, April 8, 2004.
37. Kamisky D. Process for the preparation of substituted pyrano(3,2-c)(1,2)benzo-thiazine 6,6-dioxides. U. S. Patent US3898218A, August 5, 1975.
38. Kamisky D.; Klutchko S. Polycyclic gamma-pyrone-3-carboxaldehyde deriva-tives U. S. Patent US3959480A, May 25, 1976.
39. Kamisky D. Polycyclic dioxaborin complexes. U. S. Patent US3936488A, February 3, 1976.
40. Kamisky D. Hydroxymethylene-substituted chromone-3-carboxaldehydes, process for their preparation and intermediates produced thereby. U. S. Patent US3936563A, February 3, 1976.
41. Kamisky D. Process for the preparation of gamma-pyrone-3-carboxaldehydes. U. S. Patent US3862144A, January 21, 1975.
42. Kamisky D.; Klutchko S. Polycyclic gamma-pyrone-3-carboxaldehyde deriva-tives. U. S. Patent US3887585A, June 3, 1975.
43. House, H. O.; Reif, D. J. The Rearrangement of α,β-Epoxy Ketones. II. Migratory Aptitudes 1. *J. Am. Chem. Soc.* **1955**, *77* (24), 6525–6532. https://doi.org/10.1021/ja01629a035.
44. House, H. O.; Reif, D. J. The Rearrangement of α,β-Epoxy Ketones. VII. The α-Ethylbenzalacetophenone Oxide System. *J. Am. Chem. Soc.* **1957**, *79* (24), 6491–6495. https://doi.org/10.1021/ja01581a035.
45. House, H. O.; Ryerson, G. D. The Rearrangement of α,β-Epoxy Ketones. VIII. Effect of Substituents on the Rate of Rearrangement. *J. Am. Chem. Soc.* **1961**, *83* (4), 979–983. https://doi.org/10.1021/ja01465a052.
46. Brown, N. M. D.; Bladon, P. Spectroscopy and Structure of (1,3-Diketonato)Boron Difluorides and Related Compounds. *J. Chem. Soc. A* **1969**, 526. https://doi.org/10.1039/j19690000526.
47. Fabian, J.; Hartmann, H. 1,3,2-Dioxaborines as Potential Components in Advanced Materials-a Theoretical Study on Electron Affinity. *J. Phys. Org. Chem.* **2004**, *17* (5), 359–369. https://doi.org/10.1002/poc.736.
48. Giron, R. G. P.; Ferguson, G. S. Tetrafluoroborate and Hexafluorophosphate Ions Are Not Interchangeable: A Density Functional Theory Comparison of Hydrogen Bonding. *ChemistrySelect* **2017**, *2* (33), 10895–10901. https://doi.org/10.1002/SLCT.201702176.
49. Schleyer, P. von R.; Maerker, C.; Dransfeld, A.; Jiao, H.; van Eikema Hommes, N. J. R. Nucleus-Independent Chemical Shifts: A Simple and Efficient Aromaticity Probe. *J. Am. Chem. Soc.* **1996**, *118* (26), 6317–6318. https://doi.org/10.1021/ja960582d.
50. Borisenko, A. V.; Vovna, V. I.; Gorachakov, V. V.; Korotkikh, O. A. Photoelectron Spectra and Electron Structures of Some Boron b-Diketonates. *J. Struct. Chem.* **1987**, *28* (1), 127–130. https://doi.org/10.1007/BF00749560.

ISSN 2308-8303 (Print) / 2518-1548 (Online)

51. Vovna, V. I.; Kazachek, M. V.; L'vov, I. B. Excited States and Absorption Spectra of β-Diketonate Complexes of Boron Difluoride with Aromatic Substituents. *Opt. Spectrosc.* **2012**, *112* (4), 497–505. https://doi.org/10.1134/S0030400X12030228.
52. Vovna, V. I.; Tikhonov, S. A.; Lvov, I. B. Photoelectron Spectra and Electronic Structure of Boron Difluoride β-Diketonates with Aromatic Substituents. *Russ. J. Phys. Chem. A* **2013**, *87* (4), 688–693. https://doi.org/10.1134/S0036024413040304.
53. Tikhonov, S. A.; Vovna, V. I. Boron Chelate Complexes: X-Ray and UV Photoelectron Spectra and Electronic Structure. *Russ. Chem. Bull.* **2018**, *67* (7), 1153–1166. https://doi.org/10.1007/s11172-018-2196-2.
54. Foris, A. On ^{19}F NMR Spectra of BF_2 and BF Complexes and Related Compounds, **2016**. https://doi.org/10.13140/RG.2.2.30488.60160.
55. Gillespie, R. J.; Hartman, J. S. Change of Sign of the Boron–Fluorine Spin–Spin Coupling Constant in the Tetrafluoroborate Anion. *J. Chem. Phys.* **1966**, *45* (7), 2712–2713. https://doi.org/10.1063/1.1728005.
56. Tay, A. C. Y.; Frogley, B. J.; Ware, D. C.; Brothers, P. J. Boron Calixphyrin Complexes: Exploring the Coordination Chemistry of a BODIPY/Porphyrin Hybrid. *Dalton Trans.* **2018**, *47* (10), 3388–3399. https://doi.org/10.1039/C7DT04575A.
57. Minkin, V. I. Glossary of Terms Used in Theoretical Organic Chemistry. *Pure Appl. Chem.* **1999**, *71* (10), 1919–1981. https://doi.org/10.1351/pac199971101919.
58. Desfrançois, C.; Périquet, V.; Lyapustina, S. A.; Lippa, T. P.; Robinson, D. W.; Bowen, K. H.; Nonaka, H.; Compton, R. N. Electron Binding to Valence and Multipole States of Molecules: Nitrobenzene, Para- and Meta-Dinitrobenzenes. *J. Chem. Phys.* **1999**, *111* (10), 4569–4576. https://doi.org/10.1063/1.479218.
59. Chowdhury, S.; Kebarle, P. Electron Affinities of Di- and Tetracyanoethylene and Cyanobenzenes Based on Measurements of Gas-Phase Electron-Transfer Equilibria. *J. Am. Chem. Soc.* **1986**, *108* (18), 5453–5459. https://doi.org/10.1021/JA00278A014/ASSET/JA00278A014.FP.PNG_V03.
60. Görlitz, G.; Hartmann, H.; Kossanyi, J.; Valat, P.; Wintgens, V. Spectroscopic Anomalies in the 4-Aryl-2,2-Difluoro-6-Methyl-1,3,2-Dioxaborine Series. *Berichte der Bunsengesellschaft für physikalische Chemie* **1998**, *102* (10), 1449–1458. https://doi.org/10.1002/bbpc.199800013.
61. Xu, S.; Evans, R. E.; Liu, T.; Zhang, G.; Demas, J. N.; Trindle, C. O.; Fraser, C. L. Aromatic Difluoroboron β-Diketonate Complexes: Effects of π-Conjugation and Media on Optical Properties. *Inorg. Chem.* **2013**, *52* (7), 3597–3610. https://doi.org/10.1021/IC300077G/SUPPL_FILE/IC300077G_SI_001.PDF.
62. Kulinich, A. V; Ishchenko, A. A. Merocyanine Dyes: Synthesis, Structure, Properties and Applications. *Russ. Chem. Rev.* **2009**, *78* (2), 141–164. https://doi.org/10.1070/RC2009v078n02ABEH003900.
63. Sturmer, D. M. Synthesis and Properties of Cyanine and Related Dyes. In *Chemistry of Heterocyclic Compounds: Special Topics in Heterocyclic Chemistry, Volume 30*; Weissberger, A; Taylor, E. C., Eds.; John Wiley & Sons: New York, 1977; pp. 441–587.
64. Dähne, S. Color and Constitution: One Hundred Years of Research. *Science* **1978**, *199* (4334), 1163–1167. https://doi.org/10.1126/science.199.4334.1163.
65. Bach, G.; Daehne, S. Chapter 15 – Cyanine dyes and related compounds. In *Second Supplements to the 2nd Edition of Rodd's Chemistry of Carbon Compounds, Volume IV*; Sainsbury, M. Ed.; Elsevier: Amsterdam, 1997; pp. 383–481. https://doi.org/10.1016/B978-044453347-0.50165-8.
66. Lawrentz, U.; Grahn, W.; Lukaszuk, K.; Klein, C.; Wortmann, R.; Feldner, A.; Scherer, D. Donor-Acceptor Oligoenes with a Locked All-Trans Conformation: Synthesis and Linear and Nonlinear Optical Properties. *Chem. - Eur. J.* **2002**, *8* (7), 1573–1590. https://doi.org/10.1002/1521-3765(20020402)8:7<1573::AID-CHEM1573>3.0.CO;2-T.
67. Ishchenko, A. A.; Kulinich, A. V.; Bondarev, S. L.; Knyukshto, V. N. Photodynamics of Polyene–Polymethine Transformations and Spectral Fluorescent Properties of Merocyanine Dyes. *J. Phys. Chem. A* **2007**, *111* (51), 13629–13637. https://doi.org/10.1021/jp076016u.
68. Zhang, X.; Tian, Y.; Li, Z.; Tian, X.; Sun, H.; Liu, H.; Moore, A.; Ran, C. Design and Synthesis of Curcumin Analogues for in Vivo Fluorescence Imaging and Inhibiting Copper-Induced Cross-Linking of Amyloid Beta Species in Alzheimer's Disease. *J. Am. Chem. Soc.* **2013**, *135* (44), 16397–16409. https://doi.org/10.1021/ja405239v.
69. Gustav, K.; Bartsch, U.; Günther, W. Spektroskopische Untersuchungen an Organischen Carbonylverbindungen, 10. Mitt.: Vergleichende Absorptions-, Fluoreszenz- Und NMR-Messungen an Ausgewählten β-Diketonen Und Ihren BF_2- Und Be-Komplexen. *Monatshefte für Chemie / Chemical Monthly* **1994**, *125* (12), 1321–1325. https://doi.org/10.1007/BF00811081.
70. D'Aléo, A.; Gachet, D.; Heresanu, V.; Giorgi, M.; Fages, F. Efficient NIR-Light Emission from Solid-State Complexes of Boron Difluoride with 2'-Hydroxychalcone Derivatives. *Chem. – Eur. J.* **2012**, *18* (40), 12764–12772. https://doi.org/10.1002/CHEM.201201812.
71. D'Aléo, A.; Felouat, A.; Fages, F. Boron Difluoride Complexes of 2'-Hydroxychalcones and Curcuminoids as Fluorescent Dyes for Photonic Applications. *Adv. Nat. Sci.: Nanosci. Nanotechnol.* **2014**, *6* (1), 015009. https://doi.org/10.1088/2043-6262/6/1/015009.
72. Park, K. S.; Kim, M. K.; Seo, Y.; Ha, T.; Yoo, K.; Hyeon, S. J.; Hwang, Y. J.; Lee, J.; Ryu, H.; Choo, H.; Chong, Y. A Difluoroboron β-Diketonate Probe Shows "Turn-on" Near-Infrared Fluorescence Specific for Tau Fibrils. *ACS Chem. Neurosci.* **2017**, *8* (10), 2124–2131. https://doi.org/10.1021/acschemneuro.7b00224.
73. Traven, V. F.; Chibisova, T. A.; Manaev, A. V. Polymethine Dyes Derived from Boron Complexes of Acetylhydroxycoumarins. *Dyes Pigm.* **2003**, *58* (1), 41–46. https://doi.org/10.1016/S0143-7208(03)00022-6.
74. Gerasov, A. O.; Shandura, M. P.; Kovtun, Y. P. Polymethine Dyes Derived from the Boron Difluoride Complex of 3-Acetyl-5,7-Di(Pyrrolidin-1-yl)-4-Hydroxycoumarin. *Dyes Pigm.* **2008**, *79* (3), 252–258. https://doi.org/10.1016/j.dyepig.2008.03.005.
75. Gerasov, A. O.; Zyabrev, K. V.; Shandura, M. P.; Kovtun, Y. P. The Structural Criteria of Hydrolytic Stability in Series of Dioxaborine Polymethine Dyes. *Dyes Pigm.* **2011**, *89* (1), 76–85. https://doi.org/10.1016/j.dyepig.2010.09.007.
76. Zyabrev, K.; Dekhtyar, M.; Vlasenko, Y.; Chernega, A.; Slominskii, Y.; Tolmachev, A. New 2,2-Difluoro-1,3,2(2H)Oxazaborines and Merocyanines Derived from Them. *Dyes Pigm.* **2012**, *92* (1), 749–757. https://doi.org/10.1016/J.DYEPIG.2011.05.025.
77. Traven, V. F.; Manaev, A. V.; Bochkov, A. Y.; Chibisova, T. A.; Ivanov, I. V. New Reactions, Functional Compounds, and Materials in the Series of Coumarin and Its Analogs. *Russ. Chem. Bull.* **2012**, *61* (7), 1342–1362. https://doi.org/10.1007/s11172-012-0179-2.
78. Gerasov, A. O.; Shandura, M. P.; Kovtun, Y. P. Series of Polymethine Dyes Derived from 2,2-Difluoro-1,3,2-(2H)-Dioxaborine of 3-Acetyl-7-Diethylamino-4-Hydroxycoumarin. *Dyes Pigm.* **2008**, *77* (3), 598–607. https://doi.org/10.1016/j.dyepig.2007.08.013.
79. Halik, M.; Hartmann, H. Synthesis and Characterization of New Long-Wavelength-Absorbing Oxonol Dyes from the 2,2-Difluoro-1,3,2-Dioxaborine Type. *Chem. – Eur. J.* **1999**, *5* (9), 2511–2517. https://doi.org/10.1002/(SICI)1521-3765(19990903)5:9<2511::AID-CHEM2511>3.0.CO;2-6.

80. Zyabrev, K.; Doroshenko, A.; Mikitenko, E.; Slominskii, Y.; Tolmachev, A. Design, Synthesis, and Spectral Luminescent Properties of a Novel Polycarbocyanine Series Based on the 2,2-Difluoro-1,3,2-Dioxaborine Nucleus. *Eur. J. Org. Chem.* **2008**, *2008* (9), 1550–1558. https://doi.org/10.1002/EJOC.200701012.
81. Lin, H. C.; Kim, H.; Barlow, S.; Hales, J. M.; Perry, J. W.; Marder, S. R. Synthesis and Linear and Nonlinear Optical Properties of Metal-Terminated Bis(Dioxaborine) Polymethines. *Chem. Commun.* **2010**, *47* (2), 782–784. https://doi.org/10.1039/C0CC02003F.
82. Matichak, J. D.; Hales, J. M.; Barlow, S.; Perry, J. W.; Marder, S. R. Dioxaborine- and Indole-Terminated Polymethines: Effects of Bridge Substitution on Absorption Spectra and Third-Order Polarizabilities. *J. Phys. Chem. A* **2011**, *115* (11), 2160–2168. https://doi.org/10.1021/jp110425r.
83. Zyabrev, K. V.; Il'chenko, A. Y.; Slominskii, Y. L.; Rimanov, N. N.; Tolmachev, A. I. Polymethine Dyes Derived from 2,2-Difluoro-3,1,2-(2H)-Oxaoxoniaboratines with Polymethylene Bridge Groups in the Chromophore. *Dyes Pigm.* **2006**, *71* (3), 199–206. https://doi.org/10.1016/J.DYEPIG.2005.07.006.
84. Rajeshirke, M.; Tathe, A. B.; Sekar, N. Viscosity Sensitive Fluorescent Coumarin-Carbazole Chalcones and Their BF2 Complexes Containing Carboxylic Acid – Synthesis and Solvatochromism. *J. Mol. Liq.* **2018**, *264*, 358–366. https://doi.org/10.1016/J.MOLLIQ.2018.05.074.
85. Sun, Q.; Wang, W.; Chen, Z.; Yao, Y.; Zhang, W.; Duan, L.; Qian, J. A Fluorescence Turn-on Probe for Human (Bovine) Serum Albumin Based on the Hydrolysis of a Dioxaborine Group Promoted by Proteins. *Chem. Commun.* **2017**, *53* (48), 6432–6435. https://doi.org/10.1039/C7CC03587J.
86. Zhou, J.; Jangili, P.; Son, S.; Ji, M. S.; Won, M.; Kim, J. S. Fluorescent Diagnostic Probes in Neurodegenerative Diseases. *Adv. Mater.* **2020**, *32* (51), 2001945. https://doi.org/10.1002/ADMA.202001945.
87. Yang, J.; Zeng, F.; Li, X.; Ran, C.; Xu, Y.; Li, Y. Highly Specific Detection of Aβ Oligomers in Early Alzheimer's Disease by a near-Infrared Fluorescent Probe with a "V-Shaped" Spatial Conformation. *Chem. Commun.* **2020**, *56* (4), 583–586. https://doi.org/10.1039/C9CC08894F.
88. Zhou, Y.; Chen, Y. Z.; Cao, J. H.; Yang, Q. Z.; Wu, L. Z.; Tung, C. H.; Wu, D. Y. Dicyanoboron Diketonate Dyes: Synthesis, Photophysical Properties and Bioimaging. *Dyes Pigm.* **2015**, *112*, 162–169. https://doi.org/10.1016/J.DYEPIG.2014.07.001.
89. Dewar, M. J. S. 478. Colour and Constitution. Part I. Basic Dyes. *J. Chem. Soc.* **1950**, 2329. https://doi.org/10.1039/jr9500002329.
90. Knott, E. B. 227. The Colour of Organic Compounds. Part I. A General Colour Rule. *J. Chem. Soc.* **1951**, 1024. https://doi.org/10.1039/jr9510001024.
91. Borysyuk, V. I.; Yashchuk, V. M.; Naumenko, A. P.; Stanova, A. V.; Gerasova, V. G.; Gerasov, A. O.; Kovtun, Y. P.; Shandura, M. P.; Kachkovsky, O. D. Influence of Surplus Negative Charge on Absorption and Fluorescence Excitation Spectra of Asymmetric Polymethine Dyes. *Ukr. J. Phys.* **2015**, *60* (7), 593-600-593–600. https://doi.org/10.15407/ujpe60.07.0593.
92. Gerasov, A. O.; Shandura, M. P.; Kovtun, Y. P.; Kachkovsky, A. D. The Nature of Electron Transitions in Anionic Dioxaborines, Derivatives of Aminocoumarin. *J. Phys. Org. Chem.* **2008**, *21* (5), 419–425. https://doi.org/10.1002/POC.1368.
93. Tyutyulkov, N.; Fabian, J.; Mehlhorn, A.; Dietz, F.; Tadjer, A. in *Polymethine Dyes. Structure and Properties*; Peters, A. T., Ed.; St. Kliment Ohridski Univer-sity Pres; Sofia, **1991**; pp. 67–68.
94. Uranga-Barandiaran, O.; Catherin, M.; Zaborova, E.; D'Aléo, A.; Fages, F.; Castet, F.; Casanova, D. Optical Properties of Quadrupolar and Bi-Quadrupolar Dyes: Intra and Inter Chromophoric Interactions. *Phys. Chem. Chem. Phys.* **2018**, *20* (38), 24623–24632. https://doi.org/10.1039/C8CP05048A.
95. Dirk, C. W.; Herndon, W. C.; Cervantes-Lee, F.; Selnau, H.; Martinez, S.; Kalamegham, P.; Tan, A.; Campos, G.; Velez, M. Squarylium Dyes: Structural Factors Pertaining to the Negative Third-Order Nonlinear Optical Response. *J. Am. Chem. Soc.* **1995**, *117* (8), 2214–2225. https://doi.org/10.1021/ja00113a011.
96. Terenziani, F.; Painelli, A.; Katan, C.; Charlot, M.; Blanchard-Desce, M. Charge Instability in Quadrupolar Chromophores: Symmetry Breaking and Solvatochromism. *J. Am. Chem. Soc.* **2006**, *128* (49), 15742–15755. https://doi.org/10.1021/ja064521j.
97. Ran, C.; Xu, X.; Raymond, S. B.; Ferrara, B. J.; Neal, K.; Bacskai, B. J.; Medarova, Z.; Moore, A. Design, Synthesis, and Testing of Difluoroboron-Derivatized Curcumins as Near-Infrared Probes for in Vivo Detection of Amyloid-β Deposits. *J. Am. Chem. Soc.* **2009**, *131* (42), 15257–15261. https://doi.org/10.1021/ja9047043.
98. Selkoe, D. J. Translating Cell Biology into Therapeutic Advances in Alzheimer's Disease. *Nature* **1999**, *399* (6738), A23–A31. https://doi.org/10.1038/399a023.
99. Li, Z.; Song, Y.; Lu, Z.; Li, Z.; Li, R.; Li, Y.; Hou, S.; Zhu, Y.-P.; Guo, H. Novel Difluoroboron Complexes of Curcumin Analogues as "Dual-Dual" Sensing Materials for Volatile Acid and Amine Vapors. *Dyes Pigm.* **2020**, *179*, 108406. https://doi.org/10.1016/j.dyepig.2020.108406.
100. Bai, G.; Yu, C.; Cheng, C.; Hao, E.; Wei, Y.; Mu, X.; Jiao, L. Syntheses and Photophysical Properties of BF_2 Complexes of Curcumin Analogues. *Org. Biomol. Chem.* **2014**, *12* (10), 1618–1626. https://doi.org/10.1039/C3OB42201A.
101. Liu, K.; Chen, J.; Chojnacki, J.; Zhang, S. BF_3·OEt_2-Promoted Concise Synthesis of Difluoroboron-Derivatized Curcumins from Aldehydes and 2,4-Pentanedione. *Tetrahedron Lett.* **2013**, *54* (16), 2070–2073. https://doi.org/10.1016/j.tetlet.2013.02.015.
102. Felouat, A.; D'Aléo, A.; Fages, F. Synthesis and Photophysical Properties of Difluoroboron Complexes of Curcuminoid Derivatives Bearing Different Terminal Aromatic Units and a Meso-Aryl Ring. *J. Org. Chem.* **2013**, *78* (9), 4446–4455. https://doi.org/10.1021/jo400389h.
103. Sherin, D. R.; Thomas, S. G.; Rajasekharan, K. N. Mechanochemical Synthesis of 2,2-Difluoro-4,6-Bis(β-Styryl)-1,3,2-Dioxaborines and Their Use in Cyanide Ion Sensing. *Heterocycl. Commun.* **2015**, *21* (6), 381–385. https://doi.org/10.1515/hc-2015-0096.
104. Rivoal, M.; Zaborova, E.; Canard, G.; D'Aléo, A.; Fages, F. Synthesis, Electrochemical and Photophysical Studies of the Borondifluoride Complex of a Meta-Linked Biscurcuminoid. *New J. Chem.* **2016**, *40* (2), 1297–1305. https://doi.org/10.1039/C5NJ00925A.
105. Canard, G.; Ponce-Vargas, M.; Jacquemin, D.; Le Guennic, B.; Felouat, A.; Rivoal, M.; Zaborova, E.; D'Aléo, A.; Fages, F. Influence of the Electron Donor Groups on the Optical and Electrochemical Properties of Borondifluoride Complexes of Curcuminoid Derivatives: A Joint Theoretical and Experimental Study. *RSC Adv.* **2017**, *7* (17), 10132–10142. https://doi.org/10.1039/C6RA25436E.
106. Kamada, K.; Namikawa, T.; Senatore, S.; Matthews, C.; Lenne, P.-F.; Maury, O.; Andraud, C.; Ponce-Vargas, M.; Le Guennic, B.; Jacquemin, D.; Agbo, P.; An, D. D.; Gauny, S. S.; Liu, X.; Abergel, R. J.; Fages, F.; D'Aléo, A. Boron Difluoride Curcuminoid Fluorophores with Enhanced Two-Photon Excited Fluorescence Emission and Versatile Living-Cell Imaging Properties. *Chem. - Eur. J.* **2016**, *22* (15), 5219–5232. https://doi.org/10.1002/chem.201504903.
107. Chaicham, A.; Kulchat, S.; Tumcharern, G.; Tuntulani, T.; Tomapatanaget, B. Synthesis, Photophysical Properties, and Cyanide Detection in Aqueous Solution of BF2-Curcumin Dyes. *Tetrahedron* **2010**, *66* (32), 6217–6223. https://doi.org/10.1016/j.tet.2010.05.088.

ISSN 2308-8303 (Print) / 2518-1548 (Online)

108. Margar, S. N.; Rhyman, L.; Ramasami, P.; Sekar, N. Fluorescent Difluoroboron-Curcumin Analogs: An Investigation of the Electronic Structures and Photophysical Properties. *Spectrochim. Acta, Part A* **2016**, *152*, 241–251. https://doi.org/10.1016/j.saa.2015.07.064.
109. Raikwar, M. M.; Rhyman, L.; Ramasami, P.; Sekar, N. Theoretical Investigation of Difluoroboron Complex of Curcuminoid Derivatives with and without Phenyl Substituent (at Meso Position): Linear and Non-Linear Optical Study. *ChemistrySelect* **2018**, *3* (40), 11339–11349. https://doi.org/10.1002/SLCT.201802231.
110. Insuasty, D.; Cabrera, L.; Ortiz, A.; Insuasty, B.; Quiroga, J.; Abonia, R. Synthesis, Photophysical Properties and Theoretical Studies of New Bis-Quinolin Curcuminoid BF2-Complexes and Their Decomplexed Derivatives. *Spectrochim. Acta, Part A* **2020**, *230*, 118065. https://doi.org/10.1016/J.SAA.2020.118065.
111. Choi, K.-R.; Kim, D. H.; Lee, Y. U.; Placide, V.; Huynh, S.; Yao, D.; Canard, G.; Zaborova, E.; Mathevet, F.; Mager, L.; Heinrich, B.; Ribierre, J.-C.; Wu, J. W.; Fages, F.; D'Aléo, A. Effect of the Electron Donating Group on the Excited-State Electronic Nature and Epsilon-near-Zero Properties of Curcuminoid-Borondifluoride Dyes. *RSC Adv.* **2021**, *11* (60), 38247–38257. https://doi.org/10.1039/D1RA08025C.
112. Zhang, X.; Tian, Y.; Yuan, P.; Li, Y.; Yaseen, M. A.; Grutzendler, J.; Moore, A.; Ran, C. A Bifunctional Curcumin Analogue for Two-Photon Imaging and Inhibiting Crosslinking of Amyloid Beta in Alzheimer's Disease. *Chem. Commun.* **2014**, *50* (78), 11550–11553. https://doi.org/10.1039/C4CC03731F.
113. Zhang, X.; Tian, Y.; Zhang, C.; Tian, X.; Ross, A. W.; Moir, R. D.; Sun, H.; Tanzi, R. E.; Moore, A.; Ran, C. Near-Infrared Fluorescence Molecular Imaging of Amyloid Beta Species and Monitoring Therapy in Animal Models of Alzheimer's Disease. *PNAS* **2015**, *112* (31), 9734–9739. https://doi.org/10.1073/pnas.1505420112.
114. Zhang, P.; Guo, Z. Q.; Yan, C. X.; Zhu, W. H. Near-Infrared Mitochondria-Targeted Fluorescent Probe for Cysteine Based on Difluoroboron Curcuminoid Derivatives. *Chin. Chem. Lett.* **2017**, *28* (10), 1952–1956. https://doi.org/10.1016/J.CCLET.2017.08.038.
115. Chen, D.; Yang, J.; Dai, J.; Lou, X.; Zhong, C.; Yu, X.; Xia, F. A Low Background D–A–D Type Fluorescent Probe for Imaging of Biothiols in Living Cells. *J. Mater. Chem. B* **2018**, *6* (32), 5248–5255. https://doi.org/10.1039/C8TB01340C.
116. Bai, B.; Yan, C.; Zhang, Y.; Guo, Z.; Zhu, W. H. Dual-Channel near-Infrared Fluorescent Probe for Real-Time Tracking of Endogenous γ-Glutamyl Transpeptidase Activity. *Chem. Commun.* **2018**, *54* (87), 12393–12396. https://doi.org/10.1039/C8CC07376G.
117. Archet, F.; Yao, D.; Chambon, S.; Abbas, M.; D'Aléo, A.; Canard, G.; Ponce-Vargas, M.; Zaborova, E.; Le Guennic, B.; Wantz, G.; Fages, F. Synthesis of Bioinspired Curcuminoid Small Molecules for Solution-Processed Organic Solar Cells with High Open-Circuit Voltage. *ACS Energy Lett.* **2017**, *2* (6), 1303–1307. https://doi.org/10.1021/acsenergylett.7b00157.
118. Sherin, D. R.; Manojkumar, T. K.; Rajasekharan, K. N. CRANAD-1 as a Cyanide Sensor in Aqueous Media: A Theoretical Study. *RSC Adv.* **2016**, *6* (101), 99385–99390. https://doi.org/10.1039/C6RA19045F.
119. Zhang, Y.; Tu, L.; Lu, L.; Li, Y.; Song, L.; Qi, Q.; Song, H.; Li, Z.; Huang, W. Screening and Application of Boron Difluoride Complexes of Curcumin as Colorimetric and Ratiometric Fluorescent Probes for Bisulfite. *Anal. Methods* **2020**, *12* (11), 1514–1521. https://doi.org/10.1039/D0AY00173B.
120. Zhao, X.; Yang, Y.; Yu, Y.; Guo, S.; Wang, W.; Zhu, S. A Cyanine-Derivative Photosensitizer with Enhanced Photostability for Mitochondria-Targeted Photodynamic Therapy. *Chem. Commun.* **2019**, *55* (90), 13542–13545. https://doi.org/10.1039/C9CC06157F.
121. Polishchuk, V.; Stanko, M.; Kulinich, A.; Shandura, M. D–π–A–π–D Dyes with a 1,3,2-Dioxaborine Cycle in the Polymethine Chain: Efficient Long-Wavelength Fluorophores. *Eur. J. Org. Chem.* **2018**, *2018* (2), 240–246. https://doi.org/10.1002/ejoc.201701466.
122. Polishchuk, V.; Kulinich, A.; Suikov, S.; Rusanov, E.; Shandura, M. 'Hybrid' Mero-Anionic Polymethines with a 1,3,2-Dioxaborine Core. *New J. Chem.* **2022**, *46* (3), 1273–1285. https://doi.org/10.1039/D1NJ05104K.
123. Polishchuk, V.; Kulinich, A.; Rusanov, E.; Shandura, M. Highly Fluorescent Dianionic Polymethines with a 1,3,2-Dioxaborine Core. *J. Org. Chem.* **2021**, *86* (7), 5227–5233. https://doi.org/10.1021/acs.joc.1c00138.
124. Polishchuk, V.; Filatova, M.; Rusanov, E.; Shandura, M. Trianionic 1,3,2-Dioxaborine-Containing Polymethines: Bright Near-Infrared Fluorophores. *Chem. – Eur. J.* **2022**. https://doi.org/10.1002/chem.202202168.

Information about the authors:
Vladyslav M. Polishchuk (*corresponding author*), Ph.D. in Chemistry, Junior Researcher, Department of Color and Structure of Organic Compounds, Institute of Organic Chemistry of the National Academy of Sciences of Ukraine, https://orcid.org/0000-0003-4396-0119; e-mail for correspondence: vlad3ds@gmail.com.
Mykola P. Shandura, Ph.D. in Chemistry, Senior Researcher, Department of Color and Structure of Organic Compounds, Institute of Organic Chemistry of the National Academy of Sciences of Ukraine; https://orcid.org/0000-0003-0896-4376.